Journal of the Franklin Institute 361 (2024) 107086

Contents lists available at ScienceDirect

Journal of the Franklin Institute

journal homepage: www.elsevier.com/locate/fi

Feedback equivalence of the chained mechanical system to the almost linear form and its use for the sustainable multi-step walking design

Sergej Čelikovský[1,*], Milan Anderle[1]

The Czech Academy of Sciences, Institute of Information Theory and Automation (ÚTIA AV ČR), 182 00 Prague 8, Czech Republic

ARTICLE INFO

Keywords:
Chained mechanical systems walking
State and feedback equivalence

ABSTRACT

The main theoretical novelty of this paper is the state and feedback equivalence of the underactuated 4-degrees of freedom planar walking-like mechanical chain system with 3 actuators to its 8-dimensional almost linear form with 3 virtual inputs. Moreover, the only residual nonlinearity vanishes on the 4-dimensional linear subspace being forward invariant when 2 of 3 virtual inputs are set to be zero. Dynamics inside that subsystem is actually the chain of 4 integrators fed by the remaining single virtual input and it can be interpreted as a rich variety of synchronous movements of torsos and legs. In such a way, the seemingly abstract and purely theoretical result can be used to design the walking-like movement during the single-support phase. The impact effect during the impulsive-like double-support phase is then attenuated by further special trajectories tuning and finite-time stabilization technique which provides the sustainable multi-step walking design. Moreover, the target walking-like trajectory is attracted by nearby trajectories. This further justify the importance and usefulness of the mentioned state and feedback equivalence. Its viability is further demonstrated by the simulations of various scenarios of the walking-like movement and the respective torsos behaviors.

1. Introduction

Planar underactuated walking, being a part of a more general study of the so-called underactuated mechanical systems [1,2], has been broadly and deeply studied during several decades. Refer to [3–7] and the references within there for a relatively recent sketch, while [8,9] can be consulted for a deeper and systematic description of the area during earlier decades.

The aim of this paper is to derive the smooth state and feedback transformations of the walking-like underactuated systems to the almost linear form and then to show that there exist a rich variety of walking-like target trajectories such that along these trajectories the respective nonlinearities vanish. These trajectories can be therefore generated using the linear dynamics properties. More specifically, the so-called **double torso biped (DTB)** will be considered, cf. Fig. 1. During those linearly generated target walking-like trajectories the DTB torsos move mutually symmetrically either in downward positions, or in upward positions. In the latter case they can mutually switch their roles after impact and relabeling, analogously as the legs do, thereby visibly imitating the inertial effect of hands movement. In such a way, we set up and prove for a particular class of systems the paradigm that the intrinsic nature of the balancing role of hands during the walking is the maintaining the equivalence to linear dynamics.

* Corresponding author.
E-mail addresses: celikovs@utia.cas.cz (S. Čelikovský), anderle@utia.cas.cz (M. Anderle).

[1] Supported by the Czech Science Foundation research grant No. 21-03689S.

https://doi.org/10.1016/j.jfranklin.2024.107086
Received 31 July 2023; Received in revised form 19 May 2024; Accepted 9 July 2024
Available online 18 July 2024

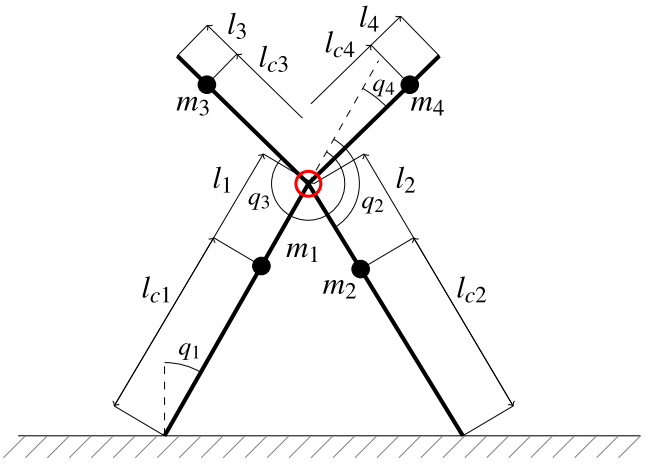

Fig. 1. DTB at the double support at the end of the step — the left leg has been the stance one. The red circle denotes the placement of the three independent actuators providing the torques u_2, u_3, u_4 actuating the so-called **directly actuated** angles q_2, q_3, q_4, respectively. The angle q_1 is the so-called **unactuated** angle.

The walking design approaches presented in the literature are either based on the stable tracking of the target hybrid periodic walking-like trajectory in the time domain [10–12], or, on the path following and orbital stability based approach used in *e.g.* [8,9,13,14]. Among various techniques to handle the walking design, the prominent role is played by the so-called **virtual holonomic constraints (VHC)**, see [15] for the detailed survey, [16] for a brief introduction and [17–20] for further theoretical study of VHC. Application of VHC to the walking design can be found in [8,9,20–24]. More special case of the VHC are the so-called **collocated VHC (CVHC)** [16,19,20,24,25]. CVHC constraint the directly actuated generalized coordinates components only, in contrast to general VHC that may constraint the unactuated components as well. CVHC are typically used for the walking design based on the time dependent target trajectory tracking, while a more general VHC rather for the path-following based design. Unlike more general VHC, the CVHC preserve the cyclic variable property of the unactuated angle at the pivot point. More specifically, for any mechanical system with n degrees of freedom and $n-1$ actuators a selection on $n-2$ CVHC gives the restricted dynamics being Lagrangian system having two degrees of freedom, one input and unactuated cyclic variable property [19]. As a consequence, such restricted dynamics is state and feedback equivalent to the single-input 4-dimensional almost linear normal form presented by Olfati-Saber in [26]. Systems with a general number of degrees of freedom and unactuated cyclic variable were studied in [27].

The only nonlinearity in the Olfati-Saber normal form is due to the $(1,1)$ entry of the inertia matrix (aka mass matrix). The idea to compute CVHC making the $(1,1)$-entry of mass matrix constant was first elaborated in [28] and then used in [29] to design the multi-step walking of the so-called **three-link (TL)** (aka biped with torso, or Compass Gait Walker with torso), known *e.g.* by studies [30,31], note also TL version with one actuator only in [14]. Yet, the respective CVHC imposed some rather restrictive conditions on system parameters to keep their invariance with respect to impact map during the double support phase of the walking. These difficulties were partly eased in [32] designing the convenient CVHC around the **downward** torso position providing far more rich collection of the desired CVHC.

The main theoretical contribution of this paper is a series of rigorous mathematical result and their proofs providing the state and feedback equivalence of the DTB to the almost linear form such that its residual nonlinearity vanishes on a specially selected submanifold, in the new coordinates being a simple 4-dimensional subspace. These results enable to abandon the VHC paradigm and rather concentrate on that equivalent form when designing the walking-like movement. Consequently, the design of a suitable target walking-like trajectory during the swing (continuous-time) phase using that equivalence is suggested. Finally, the non-smooth finite-time stabilizing feedback suppressing the tracking error during the swing phase in a settling time lower than the swing phase duration will be provided as well. In such a way, each step can be sustainably repeated again and again.

The rest of the paper is organized as follows. Some definitions and known, or straightforward, results are repeated in the next section. Section 3 rigorously formulates the main theoretical results and gives their detailed proofs. Section 4 presents the walking design based on those theoretical results including simulations. Final section draws conclusions and presents some research outlooks.

Notations. $\mathbb{Z}$ ($\mathbb{Z}^+$) denotes the set of integer (positive integer) numbers. For a smooth function $\phi(q)$, $q \in \mathbb{R}^n$, differential $\mathrm{d}\phi = \partial\phi(q)/\partial q$ is the row vector of the partial derivatives, conveniently expressed by the well-known "nabla" operator $\nabla := [\frac{\partial}{\partial q_1}, \dots, \frac{\partial}{\partial q_n}]$ as $\nabla\phi$. In the same vein, the Hessian of ϕ can be expressed as $\nabla^\top\nabla\phi$. Finally, $0_{m\times p}$, where $m, p \in \mathbb{Z}^+$, stands for $(m \times p)$ zero matrix, I_m, where $m \in \mathbb{Z}^+$, for the $(m \times m)$ identity matrix, $0_m, 1_m$ are by a context rows or columns of $m \in \mathbb{Z}^+$ zeros and ones, respectively. COM stands for the center of mass, MI for the moment of inertia and DOF for the degree(s) of freedom. The detailed glossary of other variables and notations needed during the paper technical parts is provided by the handful Table 1.

2. Definitions and preliminary results

The underactuated [1] Lagrangian system (LS) with n-DOF is given by

$$\frac{d}{dt}\left[\frac{\partial \mathscr{L}}{\partial \dot{q}}\right]^\top - \left[\frac{\partial \mathscr{L}}{\partial q}\right]^\top = \left[0_k, u_{k+1}, \dots, u_n\right]^\top, \tag{1}$$

Table 1
Glossary of used variables, parameters and other notations.

(C)VHC	(Collocated) virtual holonomic constraints
MI, DOF	Moment of inertia, degree(s) of freedom
DTB	Double torso biped
ALDTB	Almost linear equivalent DTB form
GC, GV	Generalized coordinates, generalized velocities
$q=[q_1,q_2,q_3,q_4]^\top$, $\dot q=[\dot q_1,\dot q_2,\dot q_3,\dot q_4]^\top$	DTB GC and GV defined in Fig. 1
$q^0=[q_1^0,q_2^0,q_3^0,q_4^0]^\top\in\mathbb{R}^4$	GC of the DTB "anchor" configuration
$u=[0,u_2,u_3,u_4]^\top\in\mathbb{R}^4$	DTB actuators (controlled inputs) defined in Fig. 1
$\xi=[\xi_1,\dots,\xi_8]^\top\in\mathbb{R}^8$	Transformed state variables of ALDTB
$w=[w_1,w_2,w_3]^\top\in\mathbb{R}^3$	Transformed virtual controlled inputs of ALDTB
$q^-=[q_1^-,\dots,q_4^-]^\top$, $\dot q^-=[\dot q_1^-,\dots,\dot q_4^-]^\top$	Double stance GC and GV "just before" the impact
$q^+=[q_1^+,\dots,q_4^+]^\top$, $\dot q^+=[\dot q_1^+,\dots,\dot q_4^+]^\top$	Double stance GC and GV "just after" the impact
$[\xi_1^\pm,\dots,\xi_8^\pm]^\top$	Transformed $q^\pm=[q_1^\pm,\dots,q_4^\pm]^\top$, $\dot q^\pm=[\dot q_1^\pm,\dots,\dot q_4^\pm]^\top$
$\mathscr{D}_{q^0}(q)$, $\mathscr{D}_{sw}(q)$ given by (12), (35)	Matrices to assess regularity in Theorems 3, 7
$\widehat{\mathscr{D}}_{q^0}(q)$, $\widehat{\overline{\mathscr{D}}}_{q^0}(q)$ given by (13), (14)	Matrices used for the input transformation in (15)
$\overline{\mathscr{D}}_{q^0}(q)$, given by (13)	Auxiliary matrix used during the proof of Theorem 3
m_i,l_i,l_{c_i},I_i, $i=1,\dots,4$, shown in Fig. 1	Mechanical parameters of the ith leg of the DTB
$\beta:=l_{c2}m_2l_{c3}^{-1}m_3^{-1}=l_{c1}m_1l_{c4}^{-1}m_4^{-1}$	"balancing factor" (10)
$\boldsymbol{\Phi}^{imp}(q_1,q_2,q_3,q_4)$ given by (41)	The matrix of the impact map $\dot q^+=\boldsymbol{\Phi}^{imp}(q^-)\dot q^-$
$\boldsymbol{\Phi}^{imp,\xi}(\xi_1,\xi_3,\xi_5,\xi_7)$ given by (44), (45)	The impact matrix in transformed coordinates ξ $[\xi_2^+,\xi_4^+,\xi_6^+,\xi_8^+]^\top=\boldsymbol{\Phi}^{imp,\xi}[\xi_2^-,\xi_4^-,\xi_6^-,\xi_8^-]^\top$
$[\xi_1^+,\xi_3^+,\xi_5^+,\xi_7^+]^\top=\mathscr{R}^\xi(\xi_1^-,\xi_3^-,\xi_5^-,\xi_7^-)$	The relabeling map in transformed coordinates
$D(q)$ given by (7)	DTB inertia matrix (aka mass matrix)
$d_{11}(q)$ given by (9), (10)	The $(1,1)$-entry of $D(q)$ using the balancing factor β

$$\mathscr{L}(q,\dot q)=K(q,\dot q)-V(q),\quad K(q,\dot q)=\frac{1}{2}\dot q^T D(q)\dot q. \tag{2}$$

Here, $q=(q_1,\dots,q_n)^\top$, $\dot q=(\dot q_1,\dots,\dot q_n)^\top$ are the generalized coordinates and velocities, $D(q)=D(q)^\top>0$ is the inertia matrix (aka mass matrix), while K, V are the system kinetic and potential energy. Coordinate q_i is called **cyclic variable** if D does not depend on q_i. Integer $k\geq 1$ is called the degree of the underactuation, while $u_{k+1},\dots,u_n$ are the actuators (control inputs). The coordinates $q_{k+1},\dots,q_n$ are called **(directly) actuated** while $q_1,\dots,q_k$ **unactuated**. The Eqs. (1)–(2) give

$$D(q)\ddot q+C(q,\dot q)+G(q)=\begin{bmatrix}0_k,u_{k+1},\dots,u_n\end{bmatrix}^\top, \tag{3}$$

$$G^\top(q)=\frac{\partial V(q)}{\partial q},\quad C(q,\dot q)=[C_1(q,\dot q),\dots,C_n(q,\dot q)]^\top=\left[\sum_{i=1}^n\frac{\partial D(q)}{\partial q_i}\dot q_i\right]\dot q-C_s(q,\dot q), \tag{4}$$

$$C_s^\top(q,\dot q)=\begin{bmatrix}C_{s1}(q,\dot q),\dots,C_{sn}(q,\dot q)\end{bmatrix}=\frac{\partial K(q,\dot q)}{\partial q},\quad C_{si}(q,\dot q)=\frac{1}{2}\dot q^\top\left[\frac{\partial D(q)}{\partial q_i}\right]\dot q,\ i=1,\dots,n. \tag{5}$$

Here, $G(q)$ is the gravity vector while the Coriolis terms $C(q,\dot q)$ are expressed in (4)–(5) without the usual introducing Coriolis matrix [33].

The following lemma presents the important property of the unactuated cyclic variable which was used in [26] to derive normal forms of some underactuated systems.

Lemma 1. *Consider (3)–(5) and define its generalized momenta σ_i as*

$$\sigma_i:=\frac{\partial\mathscr{L}}{\partial\dot q_i}=\frac{1}{2}\frac{\partial\dot q^\top D(q)\dot q}{\partial\dot q_i}=[0_{i-1},1,0_{n-i}]D(q)\dot q,\quad i\in\{1,\dots,n\}.$$

If q_i is unactuated cyclic variable then $\dot\sigma_i=-G_i(q)$.

Proof. It suffices to show that $\dot\sigma_i+G_i(q)=0$ when q_i is unactuated cyclic variable. To do so, realize that (3)–(5) stem from (1), (2) and therefore one has by (1) that

$$0=\frac{d}{dt}\frac{\partial\mathscr{L}}{\partial\dot q_i}-\frac{\partial\mathscr{L}}{\partial q_i}=\dot\sigma_i-\frac{\partial[K(q,\dot q)-V(q)]}{\partial q_i}=\dot\sigma_i+G_i(q).$$

Here, the first equality is by q_i being unactuated (*i.e.* $i\in\{1,\dots,k\}$), while the last one is by the left equality of (4) and q_i being cyclic (*i.e.* $\partial K(q,\dot q)/(\partial q_i)\equiv 0$). □

Planar "double torso biped" (DTB) depicted in Fig. 1 is the underactuated mechanical system having 4 degrees of freedom and 3 actuators, thereby mimicking the pair of legs without knees and two torsos mounted at their hips. The ith link ($i=1,2,3,4$) is actually a thin homogeneous rod of mass μ_i with attached point mass M_i. It is equivalently modeled by a virtual one-dimensional mass-less rigid segment having moment of inertia I_i with respect to its COM and carrying the overall mass $m_i=\mu_i+M_i$ at its center of mass (COM) indicated by the black bold bullet. Note that I_i can be straightforwardly computed from l_i,μ_i,M_i. Dynamical

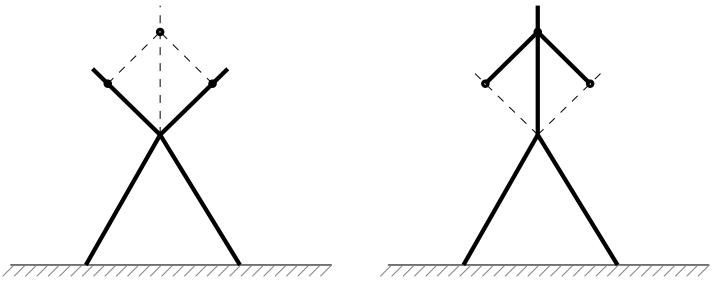

Fig. 2. DTB (on the left) as the "reduction" of the biped with single torso and hands (on the right).

model of the DTB is obtained by Euler–Lagrange formalism (ELF). More specifically, define generalized coordinates q_1, q_2, q_3, q_4 and actuators providing torques u_2, u_3, u_4 as shown in Fig. 1 and explained by its caption. Applying ELF gives

$$D(q)\ddot{q} + C(q,\dot{q}) + G(q) = \begin{bmatrix} 0 \\ u_2 \\ u_3 \\ u_4 \end{bmatrix} := u, \quad q := \begin{bmatrix} q_1 \\ q_2 \\ q_3 \\ q_4 \end{bmatrix} \in \mathbb{R}^4, \quad G = \begin{bmatrix} G_1 \\ G_2 \\ G_3 \\ G_4 \end{bmatrix}, \quad D = [d_{ij}],\ i,j = 1,\dots,4,\ D^\top = D > 0, \tag{6}$$

$$\begin{aligned} &d_{11}(q) = I_1 + I_2 + I_3 + I_4 + l_1^2 m_2 + l_1^2 m_3 + l_1^2 m_4 + l_{c1}^2 m_1 + l_{c2}^2 m_2 + l_{c3}^2 m_3 + l_{c4}^2 m_4 + 2l_1(l_{c2} m_2 \cos q_2 + l_{c3} m_3 \cos q_3 + l_{c4} m_4 \cos q_4),\\ &d_{12}(q) = m_2 l_{c2}^2 + l_1 m_2 \cos q_2 l_{c2} + I_2, \quad d_{13}(q) = m_3 l_{c3}^2 + l_1 m_3 \cos q_3 l_{c3} + I_3,\\ &d_{14}(q) = m_4 l_{c4}^2 + l_1 m_4 \cos q_4 l_{c4} + I_4, \quad d_{23}(q) = d_{24}(q) = d_{34}(q) = 0,\\ &d_{22}(q) = m_2 l_{c2}^2 + I_2,\ d_{33}(q) = m_3 l_{c3}^2 + I_3,\ d_{44}(q) = m_4 l_{c4}^2 + I_4, \end{aligned} \tag{7}$$

$$\begin{aligned} &G_1(q) = -g\left[\, l_1 m_2 \sin q_1 + l_1 m_3 \sin q_1 + l_{c1} m_1 \sin q_1 + l_{c2} m_2 \sin(q_1+q_2) + l_{c3} m_3 \sin(q_1+q_3) + l_{c3} m_3 \sin(q_1+q_4)\,\right],\\ &G_2(q) = -g l_{c2} m_2 \sin(q_1+q_2), \quad G_3(q) = -g l_{c3} m_3 \sin(q_1+q_3), \quad G_4(q) = -g l_{c4} m_4 \sin(q_1+q_4). \end{aligned} \tag{8}$$

The Coriolis terms $C(q,\dot{q})$ are determined from the inertia matrix (aka mass matrix) $D(q)$ by (4)–(5).

Assumption 2. Assume that the legs are mutually equal and the torsos are mutually equal, *i.e.* $l_1 = l_2,\ m_1 = m_2,\ l_{c1} = l_{c2},\ I_1 = I_2,\ l_3 = l_4,\ m_3 = m_4,\ l_{c3} = l_{c4},\ I_3 = I_4$. Furthermore, throughout the paper, the following more convenient expression for $d_{11}(q_2, q_3, q_4)$ of (7) will be used

$$d_{11} = \sum_{i=1}^{4} I_i + \sum_{i=2}^{4} l_1^2 m_i + \sum_{i=1}^{4} l_{ci}^2 m_i + 2l_1 l_{c3} m_3 \left[\beta \cos q_2 + \cos q_3 + \cos q_4\right], \tag{9}$$

$$\beta := l_{c2} m_2 l_{c3}^{-1} m_3^{-1} = l_{c1} m_1 l_{c4}^{-1} m_4^{-1}. \tag{10}$$

Here, β is called the **balancing factor** weighting the relative influence of the legs and the torsos.

As already noted in the introductory section, DTB may serve as an intermediate step toward more complex walking configurations having hands. More specifically, Fig. 2 compares DTB with a simple planar biped having single torso and hands on it. The latter has 5 DOF while the former has 4 DOF. Without going into the detail, conveniently selected CVHC may constraint the dynamics of that single torso and hands in such a way that resulting constraint dynamics is represented by a "virtual" DTB.

3. Main results

The main theorems on DTB state and feedback equivalence to the almost linear form will be formulated and proved in this section. To facilitate further reading of a rather technical exposition, let us start with a brief glossary of used variables, their purpose and philosophy:

1. The vector $q = [q_1, q_2, q_3, q_4]^\top \in \mathbb{R}^4$ represent the DTB generalized coordinates (angles shown in Fig. 1), while $\dot{q} = [\dot{q}_1, \dot{q}_2, \dot{q}_3, \dot{q}_4]^\top \in \mathbb{R}^4$ stands for the respective angular velocities and $u = [0, u_2, u_3, u_4]^\top \in \mathbb{R}^4$ for the input torques. Usually, the angles are assumed to belong to some set of feasible configurations denoted Q and specified if needed. Upper indices at generalized coordinates and velocities specify some selected fixed values of them.
2. To define various transformations and to assess their regularity, the matrix functions $\mathscr{D}_{q^0}(q)$, $\widehat{\mathscr{D}}_{q^0}(q)$, $\widetilde{\mathscr{D}}_{q^0}(q)$, $\overline{\mathscr{D}}_{q^0}(q)$, $\mathscr{D}_{sw}(q)$ will be defined and used. The values of all these matrices can be straightforwardly computed at any feasible configuration using the formulas given later on. **Notably**, while (4×4)-matrix $\overline{\mathscr{D}}_{q^0}(q)$ and (3×4)-matrix $\widehat{\mathscr{D}}_{q^0}(q)$ are needed to define the transformations, only (3×3)-matrices $\mathscr{D}_{q^0}(q)$ (Theorem 3) and $\mathscr{D}_{sw}(q)$ (Theorem 7) have to be checked to assess the regularity of the transformations.

3. The desired almost linear transformed system has the state variable denoted as $\xi = [\xi_1, \dots, \xi_8]^\top$ and the virtual input variable denoted as $w = [w_2, w_3, w_4]^\top$. Again, upper indices will be used to specify some fixed value of these variables.
4. The transformations will be explicitly given as the mapping from q, u variables to ξ, w variables. The key ingredient to define them is a smooth scalar function of a scalar variable denoted as $\eta_{q^0}(q_2)$, (11), along with its first and the second derivative it will appear in many other formulas.
5. Among possible fixed configurations, the key role is played by the so-called "anchor" configuration $q^0 = [q_1^0, q_2^0, q_3^0, q_4^0]^\top \in \mathbb{R}^4$ which is certain interior point of the set of feasible configurations. Its selection is rather free which will be used in the practical design later on. On a theoretical level, its selection affects the feasible set of the configurations and it should fulfill some regularity conditions.
6. Among system mechanical parameters, the crucial role is played by the balancing factor β (10) expressing the ratio between the inertia of the legs and the torsos. Value of β heavily affects the feasibility sets of transformations and thereby also target walking trajectories design later on.

To start the detailed exposition, let $q^0 = [q_1^0, q_2^0, q_3^0, q_4^0]^\top \in \mathbb{R}^4$ be the selected "anchor" configuration of DTB (6)–(8). For every $q^0 \in \mathbb{R}^4$, define the function $\eta_{q_0}(q_2) : (0, 2\pi) \mapsto \mathbb{R}$

$$\eta_{q^0}(q_2) := -\beta \sin(q_2/2) + \frac{\beta \sin^2(q_2^0/2) + \sin(q_2^0/2)\cos((q_3^0 - q_4^0)/2)}{\sin(q_2/2)}. \tag{11}$$

Note, that the only information about the model of DTB (6)–(8) used in (11) is the balancing factor β given by (10). Using $\eta_{q^0}(q_2)$ given by (11), $d_{11}(q), \dots, d_{14}(q)$ given by (7) and $G_1(q)$ given by (8), define the matrices $\mathscr{D}_{q^0}(q), \widehat{\mathscr{D}}_{q^0}(q), \widetilde{\mathscr{D}}_{q^0}(q), \overline{\mathscr{D}}_{q^0}(q)$:

$$\mathscr{D}_{q^0}(q) := \begin{bmatrix} \frac{\partial G_1}{\partial q_2}(q) - \frac{d_{12}(q)}{d_{11}(q)}\frac{\partial G_1}{\partial q_1}(q) & \frac{\partial G_1}{\partial q_3}(q) - \frac{d_{13}(q)}{d_{11}(q)}\frac{\partial G_1}{\partial q_1}(q) & \frac{\partial G_1}{\partial q_4}(q) - \frac{d_{14}(q)}{d_{11}(q)}\frac{\partial G_1}{\partial q_1}(q) \\ \frac{\eta'_{q^0}(q_2)}{(1-\eta^2_{q^0}(q_2))^{1/2}} & \frac{1}{2} & -\frac{1}{2} \\ 1 & -1 & -1 \end{bmatrix}, \tag{12}$$

$$\left.\begin{aligned} \widehat{\mathscr{D}}_{q^0}(q) &:= \begin{bmatrix} -\frac{\partial G_1}{\partial q_1}(q) & -\frac{\partial G_1}{\partial q_2}(q) & -\frac{\partial G_1}{\partial q_3}(q) & -\frac{\partial G_1}{\partial q_4}(q) \\ 0 & \frac{\eta'_{q^0}(q_2)}{(1-\eta^2_{q^0}(q_2))^{1/2}} & \frac{1}{2} & -\frac{1}{2} \\ 0 & 1 & -1 & -1 \end{bmatrix}, \quad \widetilde{\mathscr{D}}_{q^0}(q) := \widehat{\mathscr{D}}_{q^0}(q) D(q)^{-1} \begin{bmatrix} 0 & 0 & 0 \\ 1 & 0 & 0 \\ 0 & 1 & 0 \\ 0 & 0 & 1 \end{bmatrix}, \end{aligned}\right\} \tag{13}$$

$$\overline{\mathscr{D}}_{q^0}(q) := \begin{bmatrix} d_{11}(q) & d_{12}(q) & d_{13}(q) & d_{14}(q) \\ -\frac{\partial G_1}{\partial q_1}(q) & -\frac{\partial G_1}{\partial q_2}(q) & -\frac{\partial G_1}{\partial q_3}(q) & -\frac{\partial G_1}{\partial q_4}(q) \\ 0 & \frac{\eta'_{q^0}(q_2)}{(1-\eta^2_{q^0}(q_2))^{1/2}} & \frac{1}{2} & -\frac{1}{2} \\ 0 & 1 & -1 & -1 \end{bmatrix}. \tag{14}$$

For any fixed q^0, the matrices $\mathscr{D}_{q^0}(q), \widehat{\mathscr{D}}_{q^0}(q), \widetilde{\mathscr{D}}_{q^0}(q), \overline{\mathscr{D}}_{q^0}(q)$ given by (12)–(14) depend smoothly on q if $\eta_{q^0}(q_2) \neq 1$. Using (12)–(14) and (11) define the state and feedback transformation of the DTB (6)–(8), given by the mapping:

$$\left.\begin{aligned} &\mathbb{R}^{11} \mapsto \mathbb{R}^{11} : (q_1, q_2, q_3, q_4, \dot q_1, \dot q_2, \dot q_3, \dot q_4, u_2, u_3, u_4)^\top \mapsto (\xi_1, \xi_2, \xi_3, \xi_4, \xi_5, \xi_6, \xi_7, \xi_8, w_2, w_3, w_4)^\top, \\ &\xi_1 := d_{11}(q_2^0, q_3^0, q_4^0) q_1 + (m_2 l_{c2}^2 + I_2) q_2 + l_1 l_{c2} m_2 \sin q_2 + (m_3 l_{c3}^2 + I_3) q_3 + l_1 l_{c3} m_3 \sin q_3 + (m_4 l_{c4}^2 + I_4) q_4 + l_1 l_{c4} m_4 \sin q_4, \\ &\xi_3 := -G_1(q), \quad \xi_5 := \tfrac{1}{2}(q_3 - q_4) - \operatorname{acos}(\eta_{q^0}(q_2)), \quad \xi_7 := q_2 - q_3 - q_4 + \pi, \\ &\begin{bmatrix} \xi_2 \\ \xi_4 \\ \xi_6 \\ \xi_8 \end{bmatrix} = \overline{\mathscr{D}}_{q_0}(q) \begin{bmatrix} \dot q_1 \\ \dot q_2 \\ \dot q_3 \\ \dot q_4 \end{bmatrix}, \qquad \begin{bmatrix} w_2 \\ w_3 \\ w_4 \end{bmatrix} = \begin{bmatrix} -\dot q^\top \nabla^\top \nabla G_1(q) \dot q \\ \frac{\eta_{q^0}(q_2)(\eta'_{q^0}(q_2)\dot q_2)^2}{(1-\eta^2_{q^0}(q_2))^{3/2}} + \frac{\eta''_{q^0}(q_2)\dot q_2^2}{(1-\eta^2_{q^0}(q_2))^{1/2}} \\ 0 \end{bmatrix} + \widehat{\mathscr{D}}_{q_0}(q) D(q)^{-1} \left(\begin{bmatrix} 0 \\ u_2 \\ u_3 \\ u_4 \end{bmatrix} - C(q, \dot q) - G(q) \right). \end{aligned}\right\} \tag{15}$$

As a matter of fact, $\xi = [\xi_1, \dots, \xi_8]^\top$ and $w = [w_2, w_3, w_4]^\top$ serve as the state and input variables of the equivalent representation of the DTB given by the following key contribution of the paper.

Theorem 3. *Let $q^0 = [q_1^0, q_2^0, q_3^0, q_4^0]^\top$ be any DTB configuration such that*

$$\cos((q_3^0 - q_4^0)/2) > \max\left\{ -\beta \sin(q_2^0/2), -\beta \sin(q_2^0/2) + \frac{\beta - 1}{\sin(q_2^0/2)} \right\}, \tag{16}$$

$$q_2^0 + \pi = q_3^0 + q_4^0, \qquad q_2^0 \in (\pi, 2\pi), \quad q_3^0 \in (\pi, 2\pi), \quad q_4^0 \in (0, \pi), \tag{17}$$

where β is given by (10). Let Q be any set homeomorphic to $\mathbb{R}^4$ such that for some $\kappa > 0$

$$\forall q = [q_1, q_2, q_3, q_4]^\top \in Q : \ \det \mathscr{D}_{q^0}(q) \neq 0 \ \wedge \ q_2 \in (2\pi - q_2^0 - \kappa, q_2^0 + \kappa), \tag{18}$$

where $\mathscr{D}_{q^0}(q)$ is given by (12). Then the mapping $\mathbb{R}^{11} \mapsto \mathbb{R}^{11}$ defined by (15) is the diffeomorphism of $Q \times \mathbb{R}^7$ onto its image that transforms DTB (6)–(8) into the following form

$$\dot{\xi}_1 = \xi_2 - 2l_1(l_{c3}m_3 + l_{c4}m_4)\delta(\dot{q}_1, q_2, \xi_5, \xi_7),\ \dot{\xi}_2 = \xi_3,\ \dot{\xi}_3 = \xi_4,\ \dot{\xi}_4 = w_2,\ \dot{\xi}_5 = \xi_6,\ \dot{\xi}_6 = w_3,\ \dot{\xi}_7 = \xi_8,\ \dot{\xi}_8 = w_4, \tag{19}$$

where $\delta(\dot{q}_1, q_2, \xi_5, \xi_7)$ is a Lipschitz function on $\mathbb{R} \times [a, 2\pi - a] \times \mathbb{R}^2$, $\forall a \in (0, \pi)$, and

$$\delta(\dot{q}_1, q_2, 0, 0) = 0,\ \forall \dot{q}_1 \in \mathbb{R},\ \forall q_2 \in \mathbb{R}. \tag{20}$$

Remark 4. By (20) the system (19) initialized at any state with $\xi_5 = \xi_6 = \xi_7 = \xi_8 = 0$ and forced by the inputs with $w_3 \equiv 0$ and $w_4 \equiv 0$ behaves like the linear chain of four integrators $\dot{\xi}_1 = \xi_2,\ \dot{\xi}_2 = \xi_3,\ \dot{\xi}_3 = \xi_4,\ \dot{\xi}_4 = w_2$. Moreover, the transformation (15) maps the selected "anchor" configuration $q^0 = [q_1^0, q_2^0, q_3^0, q_4^0]^\top$ into the state having $\xi_5 = 0$ and $\xi_7 = 0$ while the states of the DTB (6)–(8) with $\dot{q}_2 = \dot{q}_3 = \dot{q}_4 = 0$ are mapped into the states of (19) with $\xi_6 = \xi_8 = 0$. These properties will be useful for practical walking design later on reducing it to the respective design for the linear chain of four integrators. The selection of "anchor" configuration q^0 is limited by conditions (16), (17) only. The choice of q^0 affects the transformations domain $Q \times \mathbb{R}^7$. As the main application presented in this paper later on is the swing phase target walking trajectory design and its tracking, the "anchor" configuration q^0 is not, in general, the part of the equilibrium state of the DTB (6)–(8).

Remark 5. The overall almost linearizing transformation (15) is basically determined by the choice of transformations to $\xi_1, \xi_3, \xi_5, \xi_7$, the remaining transformations to $\xi_2, \xi_4, \xi_6, \xi_8$ and w_2, w_3, w_4 result from the appropriate differentiation along trajectories to obtain the transformed system (19). Among them ξ_1, ξ_3 stem purely from the DTB model in order to use favorable properties of the unactuated cyclic variable stated by Lemma 1, while ξ_7, ξ_8 are specially selected to cancel the nonlinearity in the first equation in (19) when $\xi_5 = \xi_7 = 0$. While $\xi_7 = 0$ just ensures some suitable and simple symmetry between torsos and legs, the relation $\xi_5 = 0$ is more complex and perhaps constitutes the main novel idea of the whole paper. Indeed, any trajectory $q(t)$ contained in the subset of the state space where $\xi_5 = 0$ actually ensures that $d_{11}(q(t))$ is constant with respect to time. Recall, that $d_{11}(q)$ is given by (7) and, notably, for $\dot{q}_2 = \dot{q}_3 = \dot{q}_4 = 0$ the DTB kinetic energy is $d_{11}(q)\dot{q}_1^2/2$. The key ingredient of the overall transformation (15) is $\operatorname{acos}(\eta_{q^0}(q_2))$. As a matter of fact, $\eta_{q^0}(q_2)$ given by (11) appears in (15) only in formulas for $\xi_5, \xi_6,\ w_3$ and it ensures that $d_{11}(q_2, q_3, q_4) = d_{11}(q_2^0, q_3^0, q_4^0)\ \forall q_1, q_2, q_3, q_4$ such that $\xi_5(q_1, q_2, q_3, q_4) = 0$. The latter property reveals yet another importance of the "anchor" configuration q^0 selection discussed in Remark 4 as it determines the crucial for the further design constant value of $d_{11}(q)$. The assumption (16) is then needed for $\operatorname{acos}(\eta_{q^0}(q_2))$ to be well-defined.

Proof of Theorem 3. The definition of w_2, w_3, w_4 in (15) can be rewritten by (13) as follows

$$\begin{bmatrix} w_2 \\ w_3 \\ w_4 \end{bmatrix} = \widetilde{\mathscr{D}}_{q^0}(q) \begin{bmatrix} u_2 - C_2(q,\dot{q}) - G_2(q) \\ u_3 - C_3(q,\dot{q}) - G_3(q) \\ u_4 - C_4(q,\dot{q}) - G_4(q) \end{bmatrix} + \begin{bmatrix} -\dot{q}^\top \nabla^\top \nabla G_1(q)\dot{q} \\ \frac{\eta_{q^0}(q_2)(\eta'_{q^0}(q_2)\dot{q}_2)^2}{(1-\eta^2_{q^0}(q_2))^{3/2}} + \frac{\eta''_{q^0}(q_2)\dot{q}_2^2}{(1-\eta^2_{q^0}(q_2))^{1/2}} \\ 0 \end{bmatrix} + \Theta(q,\dot{q}), \tag{21}$$

$$\Theta(q,\dot{q}) := \widehat{\mathscr{D}}_{q^0}(q) D(q)^{-1} \left[-C_1(q,\dot{q}) - G_1(q), 0, 0, 0\right]^\top. \tag{22}$$

First, let us check that the formula for ξ_5 in (15) makes sense, *i.e.* $\eta_{q^0}(q_2) \in (-1, +1),\ \ \forall q \in Q$, needed for $\operatorname{acos}(\eta_{q^0}(q_2))$ to have real values and to be smooth. To this end, compute

$$\eta'_{q^0}(q_2) := \frac{\cos(q_2/2)}{2}\left(-\beta - \frac{\beta \sin^2(q_2^0/2) + \sin(q_2^0/2)\cos((q_3^0 - q_4^0)/2)}{\sin^2(q_2/2)}\right), \tag{23}$$

$$\begin{aligned} \eta''_{q^0}(q_2) := {} & \frac{\cos^2(q_2/2)}{2}\left(\frac{\beta \sin^2(q_2^0/2) + \sin(q_2^0/2)\cos((q_3^0 - q_4^0)/2)}{\sin^3(q_2/2)}\right) \\ & - \frac{\sin(q_2/2)}{4}\left(-\beta - \frac{\beta \sin^2(q_2^0/2) + \sin(q_2^0/2)\cos((q_3^0 - q_4^0)/2)}{\sin^2(q_2/2)}\right). \end{aligned} \tag{24}$$

By (17) it holds $q_2^0 \in (\pi, 2\pi)$ and therefore $\eta_{q^0}(\pi)$ is the unique minimum of $\eta_{q^0}(q_2)$ on $[2\pi - q_2^0, q_2^0]$. Indeed, by the assumption (16) it holds $\cos((q_3^0 - q_4^0)/2) > -\beta \sin(q_2^0/2)$ and therefore by (23) it holds $\eta'_{q^0}(q_2) < 0$ for $q_2 \in (0, \pi)$, $\eta'_{q^0}(q_2) > 0$ for $q_2 \in (\pi, 2\pi)$ and $\eta'_{q^0}(\pi) = 0$. Moreover, by (11)

$$\eta_{q^0}(\pi) = -\beta + \beta \sin^2(q_2^0/2) + \sin(q_2^0/2)\cos((q_3^0 - q_4^0)/2) > -1,$$

since $\cos((q_3^0 - q_4^0)/2) > -\beta \sin(q_2^0/2) + (\beta - 1)\sin^{-1}(q_2^0/2)$ by the assumption (16). Further, by (11) and (17) it holds $\eta_{q^0}(q_2^0) = \eta_{q^0}(2\pi - q_2^0) = \cos((q_3^0 - q_4^0)/2) \in (-1, 1)$. In such a way, $\eta_{q^0}(q_2) \in (-1, 1)\ \forall q_2 \in \{q_2^0, 2\pi - q_2^0, \pi\}$ and it has the unique minimum at π. By continuity there exists $\kappa > 0$ such that $\eta_{q^0}(q_2) \in (-1, 1)\ \forall q \in Q$ given by (18) as well.

Next, let us show that (19) holds. Using (9), (10) and the definition of ξ_1, ξ_2 in (15) one has that

$$\dot{\xi}_1 = d_{11}(q^0)\dot{q}_1 + d_{12}(q)\dot{q}_2 + d_{13}(q)\dot{q}_3 + d_{14}(q)\dot{q}_4 = [d_{11}(q_2^0, q_3^0, q_4^0) - d_{11}(q_2, q_3, q_4)]\dot{q}_1 + \xi_2 =$$
$$2l_1 l_{c3} m_3[\beta\cos q_2^0 + \cos q_3^0 + \cos q_4^0 - \beta\cos q_2 - \cos q_3 - \cos q_4]\dot{q}_1 + \xi_2 =$$
$$\xi_2 - 2l_1 l_{c3} m_3 \dot{q}_1[\beta\cos q_2 + 2\cos((q_3+q_4)/2)\cos((q_3-q_4)/2) - \beta\cos q_2^0 - \cos q_3^0 - \cos q_4^0] =$$
$$\xi_2 - 2l_1 l_{c3} m_3 \dot{q}_1[\beta\cos q_2 + 2\cos((q_2+\pi-\xi_7)/2)\cos(\operatorname{acos}(\eta(q_2)) - \xi_5) - \beta\cos q_2^0 - \cos q_3^0 - \cos q_4^0].$$

Summarizing, it holds $\dot{\xi}_1 = \xi_2 - 2l_1(l_{c3}m_3 + l_{c4}m_4)\delta(\dot{q}_1, q_2, \xi_5, \xi_7)$, where

$$\delta(\dot{q}_1, q_2, \xi_5, \xi_7) = \dot{q}_1\left[\beta\cos q_2 + 2\cos((q_2+\pi-\xi_7)/2)\cos(\operatorname{acos}(\eta_{q^0}(q_2)) - \xi_5) - \beta\cos q_2^0 - \cos q_3^0 - \cos q_4^0\right], \tag{25}$$

i.e. the first equation of (19) holds with $\delta(\dot{q}_1, q_2, \xi_5, \xi_7)$ given by (25) and such $\delta(\dot{q}_1, q_2, \xi_5, \xi_7)$ is obviously Lipschitz on $\mathbb{R}\times[a, 2\pi-a]\times\mathbb{R}^2$, $\forall a \in (0, \pi)$. To prove (20), realize that by (17), by $\cos((q_2+\pi)/2) = -\sin(q_2/2)$ and by $\cos(\operatorname{acos}(\eta_{q^0}(q_2))) = \eta_{q^0}(q_2)$ it holds

$$\delta(\dot{q}_1, q_2, 0, 0) = \dot{q}_1\left[\beta\cos q_2 + 2\cos((q_2+\pi)/2)\cos(\operatorname{acos}(\eta_{q^0}(q_2))) - \beta\cos q_2^0 - \cos q_3^0 - \cos q_4^0\right] =$$
$$\dot{q}_1\left[\beta\cos q_2 - 2\sin(q_2/2)\eta_{q^0}(q_2) - \beta\cos q_2^0 - \cos q_3^0 - \cos q_4^0\right] =$$
$$\dot{q}_1\beta\cos q_2 - 2\sin(q_2/2)\dot{q}_1\left[-\beta\sin(q_2/2) + \frac{\beta\sin^2(q_2^0/2) + \sin(q_2^0/2)\cos((q_3^0 - q_4^0)/2)}{\sin(q_2/2)}\right]$$
$$- \dot{q}_1\beta\cos q_2^0 - \dot{q}_1\cos q_3^0 - \dot{q}_1\cos q_4^0 = 0,\ \forall\dot{q}_1 \in \mathbb{R},\ \forall q_2 \in \mathbb{R},$$

where the penultimate equality is by substituting for $\eta_{q^0}(q_2)$ from (11). The last equality is due to the well-known goniometric identities. Summarizing, the first equality in (19) and (20) have been proved.

To check the second equality in (19), *i.e.* $\dot{\xi}_2 = \xi_3$, realize that q_1 is unactuated, $\xi_2 = \sigma_1$ defined in Lemma 1 formulation and $\xi_3 = -G_1(q)$ by definition of ξ_3 in (15), so that by Lemma 1 it holds $\dot{\xi}_2 = \dot{\sigma}_1 = -G_1(q) = \xi_3$. Equality $\dot{\xi}_3 = \xi_4$ is straightforward due to definition of $\xi_4 := -\nabla G_1(q)\dot{q}$ in (15) while further differentiation gives

$$\dot{\xi}_4 = -\nabla G_1 \ddot{q} - \dot{q}^\top \nabla^\top \nabla G_1(q)\dot{q}.$$

Definition of w_2 in (15) and $\ddot{q} = D(q)^{-1}[[0, u_1, u_2, u_3]^\top - C(q,\dot{q})\dot{q} - G(q)]$ (cf. (6)) then gives $\dot{\xi}_4 = w_2$. Next, one has by the definitions in (15) and by the full-time differentiation along trajectories that

$$\dot{\xi}_5 = \frac{\mathrm{d}}{\mathrm{d}t}\left[\frac{1}{2}(q_3 - q_4) - \operatorname{acos}(\eta_{q^0}(q_2))\right] = \frac{1}{2}(\dot{q}_3 - \dot{q}_4) + (1 - \eta_{q^0}^2(q_2))^{-1/2}\eta'_{q^0}(q_2)\dot{q}_2 = \xi_6,$$
$$\dot{\xi}_6 = \frac{\ddot{q}_3 - \ddot{q}_4}{2} + (1 - \eta_{q^0}^2(q_2))^{-1/2}\left[\eta'_{q^0}(q_2)\ddot{q}_2 + \eta''_{q^0}(q_2)\dot{q}_2^2\right] + (1 - \eta_{q^0}^2(q_2))^{-3/2}\eta_{q^0}(q_2)(\eta'_{q^0}(q_2)\dot{q}_2)^2$$
$$= \left[0, (1 - \eta_{q^0}^2(q_2))^{-1/2}\eta'_{q^0}(q_2), \frac{1}{2}, -\frac{1}{2}\right]D(q)^{-1}\left[[0, u_2, u_3, u_4]^\top - C(q,\dot{q})\dot{q} - G(q)\right]$$
$$+ (1 - \eta_{q^0}^2(q_2))^{-3/2}\eta_{q^0}(q_2)(\eta'_{q^0}(q_2)\dot{q}_2)^2 + (1 - \eta_{q^0}^2(q_2))^{-1/2}\eta''_{q^0}(q_2)\dot{q}_2^2 = w_3,$$

where the last equality is by the definition of w_3 in (15) and the penultimate one by

$$[\ddot{q}_1, \ddot{q}_2, \ddot{q}_3, \ddot{q}_4]^\top = D(q)^{-1}\left[[0, u_2, u_3, u_4]^\top - C(q,\dot{q})\dot{q} - G(q)\right] \tag{26}$$

stemming form (6) thereby proving both the 5th and the 6th equation in (19). Finally, one has by the definitions of ξ_7, ξ_8, w_4 in (15) and by the time differentiation that $\dot{\xi}_7 = \dot{q}_2 - \dot{q}_3 - \dot{q}_4 = \xi_8$, $\dot{\xi}_8 = \ddot{q}_2 - \ddot{q}_3 - \ddot{q}_4 = w_4$, where the last equality is again by (26). Summarizing, all equalities in (15) are valid.

For the rest of the proof the lower index indicating the "anchor" configuration q^0 will be skipped. To finish the proof, one has to show that (15) defines the mapping from $\mathbb{R}^{11}$ to $\mathbb{R}^{11}$

$$(q_1, q_2, q_3, q_4, \dot{q}_1, \dot{q}_2, \dot{q}_3, \dot{q}_4, u_2, u_3, u_4)^\top \mapsto (\xi_1, \xi_2, \xi_3, \xi_4, \xi_5, \xi_6, \xi_7, \xi_8, w_2, w_3, w_4)^\top,$$

which is smoothly invertible on the set $Q\times\mathbb{R}^7$, Q given in (18). To do so, realize that it is possible to equivalently analyze the mapping with modified order of $\xi_1, \ldots, \xi_8$, namely:

$$(q_1, q_2, q_3, q_4, \dot{q}_1, \dot{q}_2, \dot{q}_3, \dot{q}_4, u_2, u_3, u_4)^\top \mapsto (\xi_1, \xi_3, \xi_5, \xi_7, \xi_2, \xi_4, \xi_6, \xi_8, w_2, w_3, w_4)^\top$$

having at any point of the set $Q\times\mathbb{R}^7$ the following (11×11) Jacobian $\mathscr{J}(q,\dot{q})$

$$\mathscr{J}(q,\dot{q}) = \begin{bmatrix} \overline{\mathscr{D}}(q) & 0_{4\times4} & 0_{4\times3} \\ * & \overline{\mathscr{D}}(q) & 0_{4\times3} \\ * & * & \widetilde{\mathscr{D}}(q) \end{bmatrix}. \tag{27}$$

Here, $\widetilde{\mathscr{D}}$ and $\overline{\mathscr{D}}$ are (3×3) and (4×4) matrices given by (13) and (14), respectively. The straightforward row-operation elimination of $(2,1)$ entry of $\overline{\mathscr{D}}$ gives

$$\det\overline{\mathscr{D}}(q) = -d_{11}(q)\det\mathscr{D}(q), \tag{28}$$

where $\mathscr{D}$ is defined in (12). Let $\mathscr{S}$ be the (3×3) Schur complement of D

$$\mathscr{S}=\begin{bmatrix} d_{22} & d_{23} & d_{24}\\ d_{32} & d_{33} & d_{34}\\ d_{42} & d_{43} & d_{44}\end{bmatrix}-\frac{1}{d_{11}}\begin{bmatrix} d_{21}d_{12} & d_{21}d_{13} & d_{21}d_{14}\\ d_{31}d_{12} & d_{31}d_{13} & d_{31}d_{14}\\ d_{41}d_{12} & d_{41}d_{13} & d_{41}d_{14}\end{bmatrix},\ D=\begin{bmatrix} d_{11} & \dots & d_{14}\\ \vdots & \ddots & \vdots\\ d_{41} & \dots & d_{44}\end{bmatrix}, \tag{29}$$

$$D=D^{\top}>0\ \Rightarrow\ \mathscr{S}=\mathscr{S}^{\top}>0\ \Rightarrow\ \det\mathscr{S}>0. \tag{30}$$

Straightforward multiplication gives

$$\begin{bmatrix} d_{11} & d_{12} & d_{13} & d_{14}\\ d_{21} & d_{22} & d_{23} & d_{24}\\ d_{31} & d_{32} & d_{33} & d_{34}\\ d_{41} & d_{42} & d_{43} & d_{44}\end{bmatrix}\begin{bmatrix} -d_{11}^{-1}d_{12} & -d_{11}^{-1}d_{13} & -d_{11}^{-1}d_{14}\\ 1 & 0 & 0\\ 0 & 1 & 0\\ 0 & 0 & 1\end{bmatrix}=\begin{bmatrix} 0 & 0 & 0\\ 1 & 0 & 0\\ 0 & 1 & 0\\ 0 & 0 & 1\end{bmatrix}\mathscr{S}.$$

Multiplying the above equality by $\mathscr{S}^{-1}$ from the right and by D^{-1} from the left gives

$$\begin{bmatrix} d_{11} & \dots & d_{14}\\ \vdots & \ddots & \vdots\\ d_{41} & \dots & d_{44}\end{bmatrix}^{-1}\begin{bmatrix} 0 & 0 & 0\\ 1 & 0 & 0\\ 0 & 1 & 0\\ 0 & 0 & 1\end{bmatrix}=\begin{bmatrix} -d_{11}^{-1}d_{12} & -d_{11}^{-1}d_{13} & -d_{11}^{-1}d_{14}\\ 1 & 0 & 0\\ 0 & 1 & 0\\ 0 & 0 & 1\end{bmatrix}\mathscr{S}^{-1}. \tag{31}$$

Using (31), the definition of $\widetilde{\mathscr{D}}$ in (13) gives

$$\widetilde{\mathscr{D}}(q)=\begin{bmatrix} \frac{\partial G_1}{\partial q_1}(q) & \frac{\partial G_1}{\partial q_2}(q) & \frac{\partial G_1}{\partial q_3}(q) & \frac{\partial G_1}{\partial q_4}(q)\\ 0 & \frac{\eta'(q_2)}{(1-\eta^2(q_2))^{1/2}} & \frac{1}{2} & -\frac{1}{2}\\ 0 & 1 & -1 & -1\end{bmatrix}\begin{bmatrix} -d_{11}^{-1}d_{12} & -d_{11}^{-1}d_{13} & -d_{11}^{-1}d_{14}\\ 1 & 0 & 0\\ 0 & 1 & 0\\ 0 & 0 & 1\end{bmatrix}\mathscr{S}^{-1}=$$
$$\begin{bmatrix} \frac{\partial G_1}{\partial q_2}(q)-\frac{d_{12}}{d_{11}}\frac{\partial G_1}{\partial q_1}(q) & \frac{\partial G_1}{\partial q_3}(q)-\frac{d_{13}}{d_{11}}\frac{\partial G_1}{\partial q_1}(q) & \frac{\partial G_1}{\partial q_4}(q)-\frac{d_{14}}{d_{11}}\frac{\partial G_1}{\partial q_1}(q)\\ \frac{\eta'(q_2)}{(1-\eta^2(q_2))^{1/2}} & \frac{1}{2} & -\frac{1}{2}\\ 1 & -1 & -1\end{bmatrix}\mathscr{S}^{-1}=\mathscr{D}(q)\mathscr{S}^{-1},$$

where $\mathscr{D}(q)$ is defined in (12). Summarizing, it has been proved that

$$\widetilde{\mathscr{D}}(q)=\mathscr{D}(q)\mathscr{S}^{-1}\ \Rightarrow\ \det\widetilde{\mathscr{D}}(q)=\det\mathscr{D}(q)/\det\mathscr{S}. \tag{32}$$

By (27), (28), (30), (32), $d_{11}(q)>0$ and by $\det\mathscr{D}(q)\neq 0\ \forall q\in Q$ due to (18) it holds

$$\det\mathscr{J}(q,\dot q)=[d_{11}(q)]^2[\det\mathscr{D}(q)]^3/\det\mathscr{S}\neq 0\quad \forall q\in Q,\ \dot q\in\mathbb{R}^4.$$

By Global Inverse Function Theorem [34] the mapping defined by (15) is a diffeomorphism of $Q\times\mathbb{R}^7$ onto its image. Indeed, it has nonzero Jacobian on whole $Q\times\mathbb{R}^7$ which is clearly homeomorphic to $\mathbb{R}^{11}$ by assumption that Q is homeomorphic to $\mathbb{R}^4$. □

Remark 6. To follow the approach noted in Remark 4, let us analyze the possible walking-like connected smooth curves complying with $\xi_5=\xi_7=0$, which is by (15) equivalent to

$$\operatorname{acos}(\eta(q_2))=(q_3-q_4)/2,\quad q_2=q_3+q_4-\pi. \tag{33}$$

Consider DTB walking from the left to the right, its initial and final step configurations are assumed to have the same shape as shown in Figs. 3, 4 (torsos and legs are distinguished by bullets at their ends) which is needed to repeat the same step again and again. Denote the respective angles determining these double support positions at the beginning and the end of the step as $q^0=[q_1^0,q_2^0,q_3^0,q_4^0]^{\top}$ and $q^f=[q_1^f,q_2^f,q_3^f,q_4^f]^{\top}$, respectively. To apply Theorem 3, the initial configuration q^0 has to satisfy assumption (16), which is rather easy task being the pair of inequalities relating the initial angles between legs and torsos in a rather expectable way (smaller initial angle between legs allows wider range of initial torsos positions). There are two options providing the same initial and final shape:

1. The switching torsos case with $q_3^f=2\pi-q_3^0$, $q_4^f=2\pi-q_4^0$. As illustrated by Fig. 3, in this case the torsos mutually switch each other positions, analogously as legs do. Yet, such a feature obviously requires at some moment t_{sw} during the step that the torsos coincide, *i.e.* $q_3(t_{sw})=2\pi+q_4(t_{sw})$, giving by (33) that $\operatorname{acos}(\eta(q_2(t_{sw})))=\pi$, *i.e.* $\eta_{q^0}(q_2(t_{sw}))=-1$. This contradicts to the property that $\eta_{q^0}(q_2)>-1$, $\forall q\in Q$, shown during the proof of Theorem 3. As a matter of fact, the purpose of Theorem 3 is not to handle the switching torsos case, since the definition of ξ_6 in (15) clearly does not make sense for $\eta_{q^0}(q_2)=\pm 1$. The switching torsos case requires a special definition of ξ_5,ξ_6 and an extra single equality-type constraint on β,q_2^0,q_3^0,q_4^0, see Theorem 7 formulated and proved later on.

2. The non-switching torsos case with $q_3^f=2\pi-q_4^0$, $q_4^f=2\pi-q_3^0$. As illustrated by Fig. 4, in this case torsos mutually approach each other, stop before coinciding, and then recede back (note the marked torso and the marked leg). To analyze possible

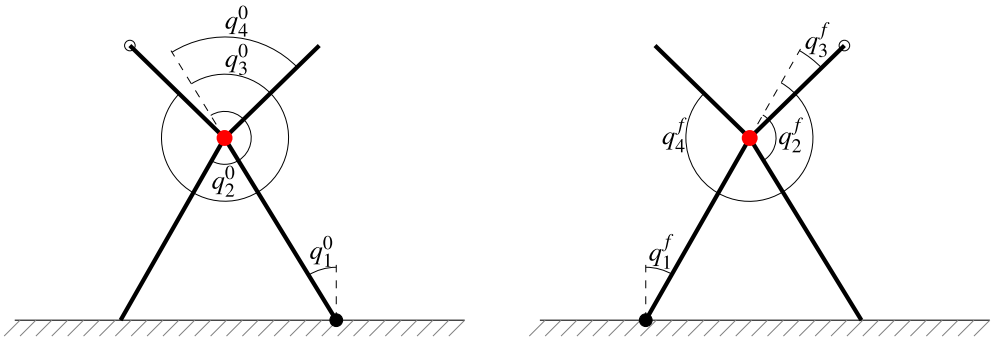

Fig. 3. DTB angles at the beginning (left) and at the end (right) of the step. Switching torsos case.

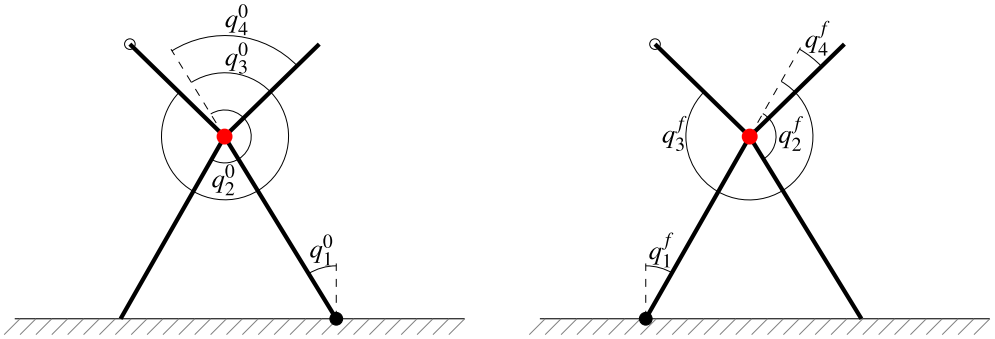

Fig. 4. DTB angles at the beginning (left) and the end (right) of the step. Non-switching torsos case.

walking-like trajectory complying with (33), realize that in Fig. 4 obviously $q_2^0 \in (\pi, 2\pi)$, $q_3^0 \in (\pi, 2\pi)$, $q_4^0 \in (0, \pi)$ which satisfy Theorem 3 assumption and imply by the straightforward triangulation, cf. Fig. 4, that

$$q_1^0 = \pi/2 - q_2^0/2, \quad q_4^0 = \pi + q_2^0 - q_3^0, \quad q_2^f = 2\pi - q_2^0, \quad q_1^f = -q_1^0.$$

Then (11) gives that $\eta_{q^0}(q_2^0) = \eta_{q^0}(q_2^f) = \cos((q_3^0 - q_4^0)/2) \in (-1, 1)$ and $\eta_{q^0}(\pi) < -1$ is a unique minimum of $\eta_{q^0}(q_2)$ on Q, as shown during the proof of Theorem 3. In such a way, for some small $\kappa > 0$ it holds $\eta_{q^0}(q_2) \in (-1, 1)\ \forall q_2 \in (q_2^f - \kappa, q_2^0 + \kappa)$, cf. (18). In such a way, in some neighborhood of a possible walking-like step starting at q_2^0 and finishing at q_2^f all transformations (15) are well defined if and only if matrix $\mathscr{D}_{q^0}(q)$ given by (12) is regular along that trajectory. This matrix can be easily computed and its determinant evaluated and Theorem 3 thereby provides a useful constructive tool to design and track walking-like trajectories during the swing phase. Such a feature will be thoroughly demonstrated later on in Section 4.4 Simulations.

To formulate the theorem enabling to handle the switching torsos case, introduce

$$\xi_5 := \frac{q_3 - q_4}{2} - \pi + \mathrm{sign}(q_2 - \pi)\left(\pi - \mathrm{acos}\left(-\beta \sin(q_2/2) + \frac{\beta - 1}{\sin(q_2/2)}\right)\right),$$

$$\xi_6 := \frac{\dot q_3 - \dot q_4}{2} + \frac{\dot q_2}{2} \frac{\beta \sin^2(q_2/2) + \beta - 1}{\sin(q_2/2)\sqrt{\beta^2 \sin^2(q_2/2) - (\beta - 1)^2}},$$

$$w_3 := \frac{1}{2}\left[0, \frac{\beta \sin^2(q_2/2) + \beta - 1}{\sin(q_2/2)\sqrt{\beta^2 \sin^2(q_2/2) - (\beta - 1)^2}}, 1, -1\right] D(q)^{-1}\left[[0, u_2, u_3, u_4]^\top - C(q, \dot q)\dot q - G(q)\right] + \theta(q_2, \dot q_2), \tag{34}$$

$$\theta(q_2, \dot q_2) := \frac{\dot q_2^2}{2} \cos(q_2/2)\left[\frac{\beta}{\sqrt{\beta^2 \sin^2(q_2/2) - (\beta - 1)^2}} - \frac{\left(\beta \sin^2(q_2/2) + \beta - 1\right)\left(4\beta^2 \sin^2(q_2/2) - 2(\beta - 1)^2\right)}{4 \sin^2(q_2/2)\left[\sqrt{\beta^2 \sin^2(q_2/2) - (\beta - 1)^2}\right]^3}\right],$$

$$\mathscr{D}_{sw}(q) := \begin{bmatrix} \frac{\partial G_1}{\partial q_2}(q) - \frac{d_{12}}{d_{11}}\frac{\partial G_1}{\partial q_1}(q) & \frac{\partial G_1}{\partial q_3}(q) - \frac{d_{13}}{d_{11}}\frac{\partial G_1}{\partial q_1}(q) & \frac{\partial G_1}{\partial q_4}(q) - \frac{d_{14}}{d_{11}}\frac{\partial G_1}{\partial q_1}(q) \\ \frac{1}{2}\frac{\beta \sin^2(q_2/2) + \beta - 1}{\sin(q_2/2)\sqrt{\beta^2 \sin^2(q_2/2) - (\beta - 1)^2}} & \frac{1}{2} & -\frac{1}{2} \\ 1 & -1 & -1 \end{bmatrix}. \tag{35}$$

Theorem 7. *Consider any* $q^0 = [q_1^0, q_2^0, q_3^0, q_4^0]^\top \in \mathbb{R}^4$ *such that* $q_3^0 \in (\pi, 2\pi)$, $q_4^0 \in (0, \pi)$ *and*

$$q_2^0 \in (\pi, q_2^m), \quad q_2^0 + \pi = q_3^0 + q_4^0, \quad \cos((q_3^0 - q_4^0)/2) = -\beta \sin(q_2^0/2) + \frac{\beta - 1}{\sin(q_2^0/2)}, \tag{36}$$

where $q_2^m := 2\pi - 2\arcsin(|1 - \beta^{-1}|)$, $\beta > \frac{1}{2}$ *and* β *is given by* (10). *Let* $\mathscr{D}_{sw}(q)$ *be given by* (35) *and* Q *be any set homeomorphic to* $\mathbb{R}^4$ *such that*

$$\forall q = [q_1, q_2, q_3, q_4]^\top \in Q: \quad \det \mathscr{D}_{sw}(q) \neq 0 \ \wedge \ q_2 \in (2\pi - q_2^m, q_2^m). \tag{37}$$

Then the mapping $\mathbb{R}^{11} \mapsto \mathbb{R}^{11}$ *defined by* (15) *with* ξ_5, ξ_6, w_3 *replaced by those of* (34) *is the diffeomorphism of* $Q \times \mathbb{R}^7$ *onto its image that transforms DTB* (6)–(8) *into* (19).

Remark 8. Theorem 7 can be used to design the DTB switching torsos type walking. First, note that the inclusion $q_2^0 \in (\pi, q_2^m)$, $q_2^m := 2\pi - 2\arcsin(|1 - \beta^{-1}|)$ required by (36) defines a nonempty range to select q_2^0 due to the theorem assumption $\beta > 1/2$ assuring $q_2^m \in (\pi, 2\pi)$. The relation (36) is then practically used as follows: selecting $q_2^0 \in (\pi, q_2^m)$ (given by the legs spreading angle at the step beginning), one has to choose proper q_3^0, q_4^0 to satisfy the equalities in (36) (giving the torsos positions at the step beginning). As it will be seen at the beginning of the proof of Theorem 7 below, $q_2^m \in (\pi, 2\pi)$ guarantees that $-\beta \sin(\frac{q_2^0}{2}) + (\beta - 1)/\sin(\frac{q_2^0}{2}) \in (-1, 1)$, *i.e.* there obviously exist $q_3^0 \in (\pi, 2\pi)$, $q_4^0 \in (0, \pi)$ satisfying $\cos(\frac{q_3^0 - q_4^0}{2}) = -\beta \sin(\frac{q_2^0}{2}) + (\beta - 1)/\sin(\frac{q_2^0}{2})$.

Further, recall that our goal is to design a switching torsos step with $q_3(t_{sw}) = 2\pi + q_4(t_{sw})$ at some time moment t_{sw} during the step while staying inside constraints $\xi_5 = \xi_7 = 0$. By definition of ξ_5 in (34) equality $\xi_5 = 0$, gives

$$\frac{q_3 - q_4}{2} = \pi - \text{sign}(q_2 - \pi)\left(\pi - \text{acos}\left(-\beta \sin(q_2/2) + \frac{\beta - 1}{\sin(q_2/2)}\right)\right) \implies$$
$$-\beta \sin(q_2(t_{sw})/2) + \frac{\beta - 1}{\sin(q_2(t_{sw})/2)} = -1 \implies \sin(q_2(t_{sw})/2) = \pm 1,$$

giving inside the range (37) the only option $q_2(t_{sw}) = \pi$. In other words, **when torsos coincide to switch each other, the legs should also coincide to switch each other.** Finally, $\xi_7 = 0$ gives by (15) $q_2 + \pi = q_3 + q_4$, *i.e.* the angle between legs and the angle between torsos have all the time common axis. In particular, the shapes at the double stance positions both at the beginning and the end of the step should be identical, which is needed anyway to repeat the same step again and again.

Proof of Theorem 7. First, let us prove that the argument of acos in (34) belongs to $[-1, 1)$ when $q \in Q$ given by (37) and therefore ξ_5 is well-defined. Denoting $x := \sin(\frac{q_2}{2})$ the previous claim equals to showing that $-\beta x + (\beta - 1)/x \in [-1, 1)$. For $x \neq 1$ and $x > 0$ it holds

$$-\beta x + (\beta - 1)/x \in (-1, 1) \ \Leftrightarrow \ -\beta x^2 + (\beta - 1) \in (-x, x) \iff$$
$$x - \beta x^2 + (\beta - 1) > 0 \ \wedge \ -x - \beta x^2 + (\beta - 1) < 0 \iff$$
$$-\beta(x - 1)(x + 1) + (x - 1) > \ \wedge \ -\beta(x - 1)(x + 1) - (x + 1) < 0 \iff$$
$$\beta(x + 1) + 1 > 0 \ \wedge \ -\beta(x - 1) - 1 < 0 \iff x > -(1 - \beta^{-1}) \ \wedge \ x \geq 1 - \beta^{-1} \iff x > |1 - \beta^{-1}|,$$

while for $x = 1$ obviously $-\beta x + (\beta - 1)/x = -1$. Realize that $x := \sin(\frac{q_2}{2})$, the inclusion in (36) and $q \in Q$ given by (37) imply straightforwardly that $1 \geq x > |1 - \beta^{-1}|$, so that, indeed, $-\beta x + (\beta - 1)/x \in [-1, 1)$ holds.

Secondly, let us show that the relations (34) imply the first and the second equality in the second row of (19), *i.e.* $\dot{\xi}_5 = \xi_6$, $\dot{\xi}_6 = w_3$. Since $\sin(q_2/2) > 0$ for $q_2 \in (0, 2\pi)$, it holds for $q_2 \neq \pi$, $q_2 \in (0, 2\pi)$, that

$$\dot{\xi}_5 = \frac{\dot{q}_3 - \dot{q}_4}{2} + \frac{\text{sign}(q_2 - \pi)[-\beta - (\beta - 1)\sin^{-2}(q_2/2)]}{\sqrt{1 - \left(-\beta \sin(q_2/2) + (\beta - 1)(\sin(q_2/2))^{-1}\right)^2}}\left[\cos\frac{q_2}{2}\right]\frac{\dot{q}_2}{2} =$$
$$\frac{\dot{q}_3 - \dot{q}_4}{2} + \frac{\text{sign}(q_2 - \pi)[-\beta \sin^2(q_2/2) - (\beta - 1)]}{\sin(q_2/2)\sqrt{\sin^2(q_2/2) - \left(-\beta \sin^2(q_2/2) + (\beta - 1)\right)^2}}\left[\cos\frac{q_2}{2}\right]\frac{\dot{q}_2}{2}.$$

Note, that

$$\sin^2(q_2/2) - \left(-\beta \sin^2(q_2/2) + (\beta - 1)\right)^2 = \sin^2(q_2/2) - \beta^2 \sin^4(q_2/2) - (\beta - 1)^2 + 2\beta^2 \sin^2(q_2/2) - 2\beta \sin^2(q_2/2) =$$
$$(1 - 2\beta + 2\beta^2)\sin^2(q_2/2) - \beta^2 \sin^4(q_2/2) - (\beta - 1)^2 = ((\beta - 1)^2 + \beta^2)\sin^2(q_2/2) - \beta^2 \sin^4(q_2/2) - (\beta - 1)^2 =$$
$$\left(1 - \sin^2(q_2/2)\right)\left(\beta^2 \sin^2(q_2/2) - (\beta - 1)^2\right)$$

and therefore

$$\dot{\xi}_5 = \frac{\dot{q}_3 - \dot{q}_4}{2} + \frac{\operatorname{sign}(q_2-\pi)\left[-\beta\sin^2(q_2/2) - (\beta-1)\right]\cos(q_2/2)}{\sin(q_2/2)\sqrt{\left(1-\sin^2(q_2/2)\right)\left(\beta^2\sin^2(q_2/2) - (\beta-1)^2\right)}}\frac{\dot{q}_2}{2} =$$
$$\frac{\dot{q}_3 - \dot{q}_4}{2} + \frac{\dot{q}_2}{2}\frac{-\beta\sin^2(q_2/2) - (\beta-1)}{\sin(q_2/2)\sqrt{\beta^2\sin^2(q_2/2) - (\beta-1)^2}}\frac{\operatorname{sign}(q_2-\pi)\cos(q_2/2)}{|\cos(q_2/2)|} =$$
$$\frac{\dot{q}_3 - \dot{q}_4}{2} + \frac{\dot{q}_2}{2}\frac{\beta\sin^2(q_2/2) + \beta - 1}{\sin(q_2/2)\sqrt{\beta^2\sin^2(q_2/2) - (\beta-1)^2}} = \xi_6,$$

where last equality is by the definition of ξ_6 in (34) and the penultimate one by

$$\operatorname{sign}(q_2-\pi)\frac{\cos(q_2/2)}{|\cos(q_2/2)|} = -1, \quad \forall q_2 \neq \pi.$$

Note, that $\beta^2\sin^2(q_2/2) - (\beta-1)^2 > 0$ by $q_2^0 \in (\pi, q_2^m)$ assumed in (36) and $q \in Q$ given by (37). In other words, we have just shown that $\dot{\xi}_5 = \xi_6$ for $q_2 \neq \pi$ and since ξ_6 equals to a smooth function of $q_2, \dot{q}_2, \dot{q}_3, \dot{q}_4$, the relation $\dot{\xi}_5 = \xi_6$ holds for $q_2 = \pi$ as well. Further

$$\dot{\xi}_6 = \frac{\ddot{q}_3 - \ddot{q}_4}{2} + \frac{\ddot{q}_2^2}{2}\frac{(\beta\sin^2(q_2/2) + \beta - 1)}{\sin(q_2/2)\sqrt{\beta^2\sin^2(q_2/2) - (\beta-1)^2}} + \frac{\dot{q}_2^2}{2}\left(\frac{\beta\sin^2(q_2/2) + \beta - 1}{\sin(q_2/2)\sqrt{\beta^2\sin^2(q_2/2) - (\beta-1)^2}}\right)'$$

and using $\ddot{q} = [\ddot{q}_1, \dots, \ddot{q}_4]^\top = D(q)^{-1}[[0, u_1, u_2]^\top - C(q,\dot{q})\dot{q} - G(q)]$ (cf. (6)) gives

$$\dot{\xi}_6 = \left[0, \frac{1}{2}\frac{\beta\sin^2(q_2/2) + \beta - 1}{\sin(q_2/2)\sqrt{\beta^2\sin^2(q_2/2) - (\beta-1)^2}}, \frac{1}{2}, -\frac{1}{2}\right]D(q)^{-1}\left[[0, u_2, u_3, u_4]^\top - C(q,\dot{q})\dot{q} - G(q)\right] +$$
$$\frac{\dot{q}_2^2}{2}\left(\frac{\beta\sin^2(q_2/2) + \beta - 1}{\sin(q_2/2)\sqrt{\beta^2\sin^2(q_2/2) - (\beta-1)^2}}\right)' = w_3,$$

where the last equality is by the definition of w_3 in (34) and by

$$\left(\frac{\beta\sin^2(q_2/2) + \beta - 1}{\sin(q_2/2)\sqrt{\beta^2\sin^2(q_2/2) - (\beta-1)^2}}\right)' =$$
$$\frac{\beta\sin(q_2/2)\cos(q_2/2)}{\sin(q_2/2)\sqrt{\beta^2\sin^2(q_2/2) - (\beta-1)^2}} + (\beta\sin^2(q_2/2) + \beta - 1)\left(\frac{1}{\sin(q_2/2)\sqrt{\beta^2\sin^2(q_2/2) - (\beta-1)^2}}\right)'.$$

In such a way, $\dot{\xi}_6 = w_3$ holds as well. To prove the remaining equalities in (19) and their properties, just repeat the respective portions of the proof of Theorem 3. Indeed, the definition of variables $\xi_1, \dots, \xi_4, w_2$ and ξ_7, ξ_8, w_4 in the current theorem are the same as in Theorem 3.

To prove the local one-to-one and smooth properties of the respective transformations, just repeat the part of the proof of Theorem 3 started by the new paragraph before (27) until end of Theorem 3 proof replacing everywhere in formulas (27)–(32) $\widetilde{\mathscr{D}}$ by $\mathscr{D}_{sw}$ and

$$\frac{\eta'(q_2)}{(1-\eta^2(q_2))^{1/2}} \quad \text{by} \quad \frac{1}{2}\frac{\beta\sin^2(q_2/2) + \beta - 1}{\sin(q_2/2)\sqrt{\beta^2\sin^2(q_2/2) - (\beta-1)^2}}.$$

This completes the proof. □

Corollary 9. *Let all assumptions of Theorem 7 hold and assume that $\beta = 1$. Then*

$$\begin{aligned} &\xi_5 = \tfrac{1}{2}(q_2 + q_3 - q_4 - 3\pi), \quad \xi_6 = \tfrac{1}{2}(\dot{q}_2 + \dot{q}_3 - \dot{q}_4), \\ &w_3 = \tfrac{1}{2}\left[0,1,1,-1\right]D(q)^{-1}\left[[0, u_2, u_3, u_4]^\top - C(q,\dot{q})\dot{q} - G(q)\right]. \end{aligned} \tag{38}$$

Moreover, the matrix $\mathscr{D}_{sw}(q)$ given by (35) becomes

$$\begin{bmatrix} \frac{\partial G_1}{\partial q_2}(q) - \frac{d_{12}}{d_{11}}\frac{\partial G_1}{\partial q_1}(q) & \frac{\partial G_1}{\partial q_3}(q) - \frac{d_{13}}{d_{11}}\frac{\partial G_1}{\partial q_1}(q) & \frac{\partial G_1}{\partial q_4}(q) - \frac{d_{14}}{d_{11}}\frac{\partial G_1}{\partial q_1}(q) \\ \frac{1}{2} & -\frac{1}{2} & \frac{1}{2} \\ 1 & -1 & -1 \end{bmatrix}. \tag{39}$$

Proof. Indeed, for $\beta = 1$ (34) gives

$$\xi_5 = \frac{q_3 - q_4}{2} - \pi + \text{sign}(q_2 - \pi)(\pi - \text{acos}\,(-\sin(q_2/2))).$$

Since $\text{acos}\,(\cos(\phi)) = 2\pi - \phi$ for $\phi \in [\pi, 2\pi]$ and $\text{acos}\,(\cos(\phi)) = \phi$ for $\phi \in [0, \pi]$, it holds

$$\text{acos}\,(-\sin(q_2/2)) = \text{acos}\,(\cos(q_2/2 + \pi/2)) = \begin{cases} (3/2)\pi - q_2/2, & q_2 \in [\pi, 2\pi] \\ q_2/2 + \pi/2, & q_2 \in [0, \pi] \end{cases}$$

and therefore $\xi_5 = (q_3 - q_4)/2 - (3/2)\pi + q_2/2\ \forall q_2 \in [0, 2\pi]$. The rest of (38) is by repeated time differentiation and by $\ddot{q} = D(q)^{-1}[[0, u_1, u_2, u_3]^\top - C(q, \dot{q})\dot{q} - G(q)]$, cf. (6). □

Remark 10. Let $\xi_5 \equiv \xi_7 \equiv 0$, where ξ_5 is given by (38) while ξ_7 by (15), *i.e.* $\xi_7 = q_2 - q_3 - q_4 + \pi \equiv 0$ and $\xi_5 = (q_2 + q_3 - q_4 - 3\pi)/2 \equiv 0$. This gives

$$q_3 = 2\pi, \quad q_4 = q_2 - \pi,\ q_2 \in [0, 2\pi].$$

The latter means, cf. Fig. 3, that the both torsos are all the time prolonging one of the legs along common line, so that walking resembles "stilts" walking. Note, that $\beta = 1$ means that inertia properties of the legs and torsos with respect to pivot point are equal. Finally, identities $\xi_5 \equiv \xi_7 \equiv 0$ are easy to enforce using feedback for $[u_2, u_3, u_4]$, since all variables $\xi_5, \dots, \xi_8$ are in this case affine dependent on $q, \dot{q}$ and the matrix (39) has constant and linearly independent the second and the third line.

4. Design of the sustainable multi-step walking based on the almost linear form

4.1. Impact map and the hybrid setting of the walking design in almost linear coordinates

It is well-known [8] that to study multi-step walking, the hybrid model setting is required. The continuous-time component of a respective hybrid system, the so-called single support (aka swing) phase is described by the system of the ordinary differential equations obtained by the Euler–Lagrange formalism and has been described in detail and investigated in the previous parts of this paper. The almost linear form has been derived for that swing phase by Theorems 3, 7 and Corollary 9. To use these results for the sustainable multi-step walking design, the behavior during the double support phase should be studied as well.

At the double support phase the walking system undergoes impulsive behavior characterized by the finite but nonzero jump of the angular velocities. This behavior then describes discrete-time component of the respective hybrid system and results in a single application of some reset of the state $(q^-, \dot{q}^-)$ at the end of the step (or, "just before" the impact) into the state $(q^+, \dot{q}^+)$ at the beginning of the next step (or "just after" the impact). While the angles remain continuously dependent on time even during the impact, the impulsive jump of velocities is expressed by the so-called **impact map**. The impact map can be obtained by the specific modeling methodology, cf. *e.g.* [8]. As both legs are assumed to be mechanically identical, to preserve the same continuous time model for the next step, the usual approach is to relabel legs in such a way that the former stance leg becomes the swing one and vice versa. This just requires to apply the so-called **relabeling map** both for angles and angular velocities, yet, relabeling map is a simple affine map. As a matter of fact, if the physical configuration of the walking-like system at the end of the step is the same as it was at the beginning of the step, the relabeling map "by definition" maps the angles at the end of the step into those present at the beginning of the step. The relabeling of the velocities is then obtained simply by the time differentiation of the relabeling of the angles. The composition of the impact and relabeling maps then results into

$$\dot{q}^+ = \boldsymbol{\Phi}^{imp}(q^-)\dot{q}^-, \quad q^\pm := (q_1^\pm, q_2^\pm, q_3^\pm, q_4^\pm)^\top, \quad \dot{q}^\pm := (\dot{q}_1^\pm, \dot{q}_2^\pm, \dot{q}_3^\pm, \dot{q}_4^\pm)^\top, \tag{40}$$

$$\boldsymbol{\Phi}^{imp}(q_1, q_2, q_3, q_4) = \begin{bmatrix} \phi_{11}(q) & \phi_{12}(q) & \phi_{13}(q) & \phi_{14}(q) \\ \phi_{21}(q) & \phi_{22}(q) & \phi_{23}(q) & \phi_{24}(q) \\ \phi_{31}(q) & \phi_{32}(q) & \phi_{33}(q) & \phi_{34}(q) \\ \phi_{41}(q) & \phi_{42}(q) & \phi_{43}(q) & \phi_{44}(q) \end{bmatrix}. \tag{41}$$

With a slight abuse of notation, the matrix $\boldsymbol{\Phi}^{imp}(q_1, q_2, q_3, q_4)$ is referred in the sequel to as the so-called **impact matrix**, though, as already noted, it actually represents composition of the impact and relabeling maps. Obtaining the impact matrix for the double-torso biped is skipped as the aim here is to present the approach how to handle it, provided it is given.

The aim of this section is to further demonstrate the usefulness of the almost linear form (19) for the multi-step walking-like movement design. To do so, the impact map has also to be studied in the ξ-coordinates $\xi_1, \dots, \xi_8$ of the form (19). More specifically, for the **switching torsos** case the representation of the impact matrix (41) in ξ-coordinates (15) modified by (34) may be obtained by the following computations

$$\begin{bmatrix} \xi_2^+ \\ \xi_4^+ \\ \xi_6^+ \\ \xi_8^+ \end{bmatrix} = \mathscr{T}^p \begin{bmatrix} \dot{q}_1^+ \\ \dot{q}_2^+ \\ \dot{q}_3^+ \\ \dot{q}_4^+ \end{bmatrix} = \mathscr{T}^p \boldsymbol{\Phi}^{imp} \begin{bmatrix} \dot{q}_1^- \\ \dot{q}_2^- \\ \dot{q}_3^- \\ \dot{q}_4^- \end{bmatrix} = \mathscr{T}^p \boldsymbol{\Phi}^{imp} [\mathscr{T}^m]^{-1} \begin{bmatrix} \xi_2^- \\ \xi_4^- \\ \xi_6^- \\ \xi_8^- \end{bmatrix},$$

$$\mathscr{T}^p = \begin{bmatrix} d_{11}(q^+) & d_{12}(q^+) & d_{13}(q^+) & d_{14}(q^+) \\ -\frac{\partial G_1}{\partial q_1}(q^+) & -\frac{\partial G_1}{\partial q_2}(q^+) & -\frac{\partial G_1}{\partial q_3}(q^+) & -\frac{\partial G_1}{\partial q_4}(q^+) \\ 0 & \frac{\beta \sin^2(q_2^+/2)+\beta-1}{2\sin(q_2^+/2)\sqrt{\beta^2\sin^2(q_2^+/2)-(\beta-1)^2}} & \frac{1}{2} & -\frac{1}{2} \\ 0 & 1 & -1 & -1 \end{bmatrix}, \tag{42}$$

$$\mathscr{T}^m = \begin{bmatrix} d_{11}(q^-) & d_{12}(q^-) & d_{13}(q^-) & d_{14}(q^-) \\ -\frac{\partial G_1}{\partial q_1}(q^-) & -\frac{\partial G_1}{\partial q_2}(q^-) & -\frac{\partial G_1}{\partial q_3}(q^-) & -\frac{\partial G_1}{\partial q_4}(q^-) \\ 0 & \frac{\beta \sin^2(q_2^-/2)+\beta-1}{2\sin(q_2^-/2)\sqrt{\beta^2\sin^2(q_2^-/2)-(\beta-1)^2}} & \frac{1}{2} & -\frac{1}{2} \\ 0 & 1 & -1 & -1 \end{bmatrix}. \tag{43}$$

The **non-switching torsos** case of Theorem 3 is analogous, the only difference for the non-switching torsos would be at $(3,2)$ entries of the matrices $\mathscr{T}^p, \mathscr{T}^m$ replaced by $\frac{\eta'_{q^0}(q_2^\pm)}{(1-\eta^2_{q^0}(q_2^\pm))^{1/2}}$. The target walking-like trajectory is assumed to undergo the impact always exactly at the prescribed double stance configuration represented uniquely both by q^+ (coordinates after relabeling), or q^- (coordinates before relabeling). Since, as just noted, q^- and q^+ are pre-selected and known, the matrices (42), (43) are considered to be constant and known. Summarizing, the impulsive component of the hybrid system is represented in ξ-coordinates as follows

$$\begin{bmatrix} \xi_2^+ \\ \xi_4^+ \\ \xi_6^+ \\ \xi_8^+ \end{bmatrix} = \boldsymbol{\Phi}^{imp,\xi} \begin{bmatrix} \xi_2^- \\ \xi_4^- \\ \xi_6^- \\ \xi_8^- \end{bmatrix}, \quad \boldsymbol{\Phi}^{imp,\xi} := \begin{bmatrix} \phi^\xi_{11} & \phi^\xi_{12} & \phi^\xi_{13} & \phi^\xi_{14} \\ \phi^\xi_{21} & \phi^\xi_{22} & \phi^\xi_{23} & \phi^\xi_{24} \\ \phi^\xi_{31} & \phi^\xi_{32} & \phi^\xi_{33} & \phi^\xi_{34} \\ \phi^\xi_{41} & \phi^\xi_{42} & \phi^\xi_{43} & \phi^\xi_{44} \end{bmatrix}, \tag{44}$$

$$\boldsymbol{\Phi}^{imp,\xi} := \mathscr{T}^p \boldsymbol{\Phi}^{imp} [\mathscr{T}^m]^{-1}, \tag{45}$$

where $\mathscr{T}^p$ and $\mathscr{T}^m$ are given by (42) and (43), respectively. In the sequel, $\boldsymbol{\Phi}^{imp,\xi}$ is called the **exact linearized impact matrix**.

Combining (44), (45) with the almost linear form given by Theorems 3 and 7 we arrive to the following cornerstone formulation of the hybrid system needed for the multi-step walking-like trajectory design in ξ-coordinates of (19):

$$\begin{aligned} &\dot\xi_1 = \xi_2 - 2l_1(l_{c3}m_3 + l_{c4}m_4)\delta(\dot q_1, q_2, \xi_5, \xi_7),\ \dot\xi_2 = \xi_3,\ \dot\xi_3 = \xi_4,\ \dot\xi_4 = w_2,\ \dot\xi_5 = \xi_6,\ \dot\xi_6 = w_3,\ \dot\xi_7 = \xi_8,\ \dot\xi_8 = w_4, \\ &\begin{bmatrix} \xi_2^+ \\ \xi_4^+ \\ \xi_6^+ \\ \xi_8^+ \end{bmatrix} = \boldsymbol{\Phi}^{imp,\xi} \begin{bmatrix} \xi_2^- \\ \xi_4^- \\ \xi_6^- \\ \xi_8^- \end{bmatrix}, \quad \begin{bmatrix} \xi_1^+ \\ \xi_3^+ \\ \xi_5^+ \\ \xi_7^+ \end{bmatrix} = \mathscr{R}^\xi(\xi_1^-, \xi_3^-, \xi_5^-, \xi_7^-), \end{aligned} \tag{46}$$

where $\mathscr{R}^\xi$ is the so-called **exact linearized relabeling map** of $(\xi_1, \xi_3, \xi_5, \xi_7)$. As the components $(\xi_1, \xi_3, \xi_5, \xi_7)$ depend on the angles q only, the same observation as for q^+, q^- applies for ξ^+, ξ^-. Namely, if the impact occurs at the given pre-required configuration identical with that of the beginning of the step, the relabeling map "automatically" returns $\xi_1^-, \xi_3^-, \xi_5^-, \xi_7^-$ into those values where the step previously started. The hybrid cyclic walking trajectory in ξ-coordinates is then obtained if one finds the solution to the above (46) such that $\xi(0) = \xi^+,\ \ \xi(T) = \xi^-$, where $T > 0$ is the time duration of the step.

To provide the hybrid cyclic design for (46) realize that

- It holds $\delta(\dot q_1, q_2, 0, 0) \equiv 0$, *i.e.* $\dot\xi_1 = \xi_2,\ \dot\xi_2 = \xi_3,\ \dot\xi_3 = \xi_4,\ \dot\xi_4 = w_2$ for $\xi_5 \equiv \xi_7 \equiv 0$.
- Identities $\xi_5 \equiv \xi_7 \equiv 0$ can be easily enforced by w_3, w_4 and these identities impose a dependence of torsos positions (angles q_3, q_4) on the swing leg position (angle q_2). Moreover, definitions of ξ_5, ξ_7 in (15) and (34) provide rich selections of those dependencies describing reasonable torsos movement during the step.

In such a way, the following two building blocks provide the overall solution to (46).

The first building block is to design a hybrid cyclic trajectory for the subsystem formed by $\xi_1, \dots, \xi_4$ only, provided identity $\xi_5 = \xi_6 = \xi_7 = \xi_8 \equiv 0$ holds all the time, *i.e.* to find the **hybrid cyclic trajectory of the four integrators chain**.

The second building block is to design the finite-time controller handling the situation when the identities $\xi_5 = \xi_6 = \xi_7 = \xi_8 \equiv 0$ do not temporarily hold.

4.2. Hybrid cyclic trajectory of the four integrators chain

Problem 11. Given $\xi_1^+, \xi_3^+, \xi_1^-, \xi_3^-$ and $T > 0$, find $\xi_2^-, \xi_4^-, \xi_2^+, \xi_4^+, w_2(t)$ such that

$$\dot\xi_1 = \xi_2,\ \dot\xi_2 = \xi_3,\ \dot\xi_3 = \xi_4,\ \dot\xi_4 = w_2, \quad \begin{bmatrix} \xi_2^+ \\ \xi_4^+ \end{bmatrix} = \begin{bmatrix} \phi^\xi_{11} & \phi^\xi_{12} \\ \phi^\xi_{21} & \phi^\xi_{22} \end{bmatrix} \begin{bmatrix} \xi_2^- \\ \xi_4^- \end{bmatrix}, \tag{47}$$

$$\xi(0)=\xi^+=[\xi_1^+,\xi_2^+,\xi_3^+,\xi_4^+]^\top\in\mathbb{R}^4,\quad \xi(T)=\xi^-=[\xi_1^-,\xi_2^-,\xi_3^-,\xi_4^-]^\top\in\mathbb{R}^4,$$

where $\phi_{11}^\xi,\phi_{12}^\xi,\phi_{21}^\xi,\phi_{22}^\xi$ are the entries of the exact linearized impact matrix (44), (45).

Proposition 12. *Assume that $T>0$, $w_2(t)=a+bt$, $a,b\in\mathbb{R}$. Denote*

$$\mathscr{C}=\begin{bmatrix} T^4/24 & T^5/120 & T & T^3/6 & 0 & 0\\ T^2/2 & T^3/6 & 0 & T & 0 & 0\\ -T^3/6 & -T^4/24 & -1 & -T^2/2 & 1 & 0\\ -T & -T^2/2 & 0 & -1 & 0 & 1\\ 0 & 0 & 1 & 0 & -\phi_{11}^\xi & -\phi_{12}^\xi\\ 0 & 0 & 0 & 1 & -\phi_{21}^\xi & -\phi_{22}^\xi \end{bmatrix}. \tag{48}$$

and assume that $\phi_{11}^\xi,\phi_{12}^\xi,\phi_{21}^\xi,\phi_{22}^\xi$ in (44) are such that $\mathscr{C}$ given by (48) is non-singular. Then for any $\xi_1^+,\xi_3^+,\xi_1^-,\xi_3^-$ Problem 11 is uniquely solved by $\xi_2^-,\xi_4^-,\xi_2^+,\xi_4^+,a,b$, where

$$\begin{bmatrix} a\\ b\\ \xi_2^+\\ \xi_4^+\\ \xi_2^-\\ \xi_4^- \end{bmatrix}=\mathscr{C}^{-1}\begin{bmatrix} \xi_1^--\xi_1^+-\xi_3^+(T^2/2)\\ \xi_3^--\xi_3^+\\ \xi_3^+T\\ 0\\ 0\\ 0 \end{bmatrix}. \tag{49}$$

Proof. One has by the repeated straightforward integration of (47)

$$\xi_4(t)=\xi_4^+ + at + b(t^2/2),\quad \xi_3(t)=\xi_3^+ + \xi_4^+ t + a(t^2/2) + b(t^3/6),$$

$$\xi_2(t)=\xi_2^+ + \xi_3^+ t + \xi_4^+(t^2/2) + a(t^3/6) + b(t^4/24),$$

$$\xi_1(t)=\xi_1^+ + \xi_2^+ t + \xi_3^+(t^2/2) + \xi_4^+(t^3/6) + a(t^4/24) + b(t^5/120).$$

Recall that solving Problem 11 requires that $\xi_2^+=\phi_{11}^\xi\xi_2^- + \phi_{12}^\xi\xi_4^-$, $\xi_4^+=\phi_{21}^\xi\xi_2^- + \xi_4^-$, $\xi(0)=\xi^+=[\xi_1^+,\xi_2^+,\xi_3^+,\xi_4^+]^\top\in\mathbb{R}^4$, $\xi(T)=\xi^-=[\xi_1^-,\xi_2^-,\xi_3^-,\xi_4^-]^\top\in\mathbb{R}^4$ and therefore

$$\mathscr{C}\begin{bmatrix} a\\ b\\ \xi_2^+\\ \xi_4^+\\ \xi_2^-\\ \xi_4^- \end{bmatrix}=\begin{bmatrix} \xi_1^- - \xi_1^+ - \xi_3^+(T^2/2)\\ \xi_3^- - \xi_3^+\\ \xi_3^+T\\ 0\\ 0\\ 0 \end{bmatrix}, \tag{50}$$

where $\mathscr{C}$ is given by (48) which straightforwardly concludes the proof. □

Importance of the solving Problem 11 is demonstrated by the following lemma.

Lemma 13. *Let be given $T>0$, $\xi_1^+\in\mathbb{R}$, $\xi_3^+\in\mathbb{R}$, $\xi_1^-\in\mathbb{R}$, $\xi_3^-\in\mathbb{R}$ and let*

$$\begin{aligned} &\xi_1^r(0)=\xi_1^+,\ \xi_2^r(0)=\xi_2^+,\ \xi_3^r(0)=\xi_3^+,\ \xi_4^r(0)=\xi_4^+,\quad w_2^r(t)=a+bt,\\ &\xi_5^r(0)=\xi_6^r(0)=\xi_7^r(0)=\xi_8^r(0)=0,\quad w_3^r(t)\equiv w_4^r(t)\equiv 0, \end{aligned} \tag{51}$$

where a,b,ξ_2^+,ξ_4^+ are given by (49). Then the system of differential equations (19) with the initial conditions $\xi^r(0)=[\xi_1^r(0),\dots,\xi_8^r(0)]^\top\in\mathbb{R}^8$ and the input $w^r(t)=[w_2^r(t),w_3^r(t),w_4^r(t)]^\top$ has the unique solution $\xi^r(t)=[\xi_1^r(t),\dots,\xi_8^r(t)]^\top$, $t\in[0,T]$, such that

$$\xi_5^r(t)\equiv\xi_6^r(t)\equiv\xi_7^r(t)\equiv\xi_8^r(t)\equiv 0,\quad \xi_1^r(T)=\xi_1^-,\ \xi_2^r(T)=\xi_2^-,\ \xi_3^r(T)=\xi_3^-,\ \xi_4^r(T)=\xi_4^-,$$

where ξ_2^-,ξ_4^- are given by (49).

Proof. Straightforward. Indeed, by the last four equations in (19) and by the lemma assumptions obviously $\xi_5^r(t)\equiv\xi_6^r(t)\equiv\xi_7^r(t)\equiv\xi_8^r(t)\equiv 0$, $\forall t\in[0,T]$. As a consequence, the first four differential equations in (19) due to $\delta(\dot q_1,q_2,0,0)=0$, $\forall\dot q_1\in\mathbb{R}$, $\forall q_2\in\mathbb{R}$ become

$$\dot\xi_1^r(t)=\xi_2^r(t),\ \dot\xi_2^r(t)=\xi_3(t),\ \dot\xi_3^r(t)=\xi_4^r(t),\ \dot\xi_4^r(t)=w_2^r(t),\ \forall t\in[0,T].$$

By their linearity and boundedness of $w_2^r(t)$ they have a unique solution $[\xi_1^r(t),\dots,\xi_8^r(t)]^\top$, $t\in[0,T]$. Moreover, using the lemma assumption (51) and Proposition 12 gives that $\xi_1^r(T)=\xi_1^-,\xi_2^r(T)=\xi_2^-,\xi_3^r(T)=\xi_3^-,\xi_4^r(T)=\xi_4^-$. □

Remark 14. Lemma 13 suggests that the solution to Problem 11 could be used to solve the task (46) if $\xi_5 \equiv \xi_6 \equiv \xi_7 \equiv \xi_8 \equiv 0$ $\forall t \in [0,T]$ which is possible if and only if $\xi_5(0) = \xi_6(0) = \xi_7(0) = \xi_8(0) = 0$, *i.e.* at the beginning of each step. Nevertheless, this requires to find $\xi_2^-, \xi_4^-, \xi_6^-, \xi_8^-, \xi_2^+, \xi_4^+, \xi_6^+, \xi_8^+$ such that

$$[\xi_2^+, \xi_4^+, 0, 0]^\top = \boldsymbol{\Phi}^{imp,\xi}[\xi_2^-, \xi_4^-, 0, 0]^\top \iff \phi_{31}^{\xi}\xi_2^- + \phi_{32}^{\xi}\xi_4^- = 0, \quad \phi_{41}^{\xi}\xi_2^- + \phi_{42}^{\xi}\xi_4^- = 0.$$

Yet, ξ_2^-, ξ_4^- are uniquely determined by Proposition 12 and therefore it is unlikely that such an additional requirement would hold. Furthermore, since $[\phi_{31}^{\xi}, \phi_{32}^{\xi}]$ and $[\phi_{41}^{\xi}, \phi_{42}^{\xi}]$ are expected to be generically linearly independent, it should have hold $\xi_2^- = \xi_4^- = 0$ unrealistically implying that all angular velocities of the DTB before the impact are zero. Moreover, this requirement is not affected by the choice of $w_2^r(t)$, *i.e.* there would be no benefit in considering more parameters in definition of $w_2^r(t)$ than used in (51).

4.3. Finite-time tracking during continuous time-phase and the overall controller design

Due to the issue mentioned by Remark 14 the situation when the identities $\xi_5 = \xi_6 = \xi_7 = \xi_8 = 0$ are violated should be somehow handled. The reference trajectory anyway provides just the open loop feed-forward which should be complemented by a tracking feedback. The latter is then capable to handle the violation of $\xi_5 = \xi_6 = \xi_7 = \xi_8 = 0$ as well. Indeed, the almost linear form (19) becomes fully linear when $\xi_5 = \xi_6 = \xi_7 = \xi_8 = 0$ and the dynamics of $\xi_5, \xi_6, \xi_7, \xi_8$ are formed by two pairs of double integrators fed by the inputs w_3, w_4, so that the **finite-time** tracking may be straightforwardly designed.

To this end, denote by $\xi^r(t) = [\xi_1^r(t), \dots, \xi_8^r(t)]^\top$, $t \in [0,T]$, a unique solution differential equations (19) with the initial conditions $\xi^r(0) = [\xi_1^r(0), \dots, \xi_8^r(0)]^\top \in \mathbb{R}^8$ and the input $w^r(t) = [w_2^r(t), w_3^r(t), w_4^r(t)]^\top$ given by (51) and let $\xi(t) \in \mathbb{R}^8$ be another solution of (19) generated by initial conditions $\xi(0) \in \mathbb{R}^8$ and the input $[w_2^{tr}, w_3^{tr}, w_3^{tr}]^\top$ to be defined later on. Further, let

$$e(t) = \xi(t) - \xi^r(t). \tag{52}$$

Realize, that $e_5 = \xi_5, e_6 = \xi_6, e_7 = \xi_7, e_8 = \xi_8$, since $\xi_5^r(t) \equiv \xi_6^r(t) \equiv \xi_7^r(t) \equiv \xi_8^r(t) \equiv 0$ and recall that by Theorem 3 it holds $\delta(\dot{q}_1, q_2, 0, 0) \equiv 0, \forall \dot{q}_1, q_2$. This obviously gives by (19)

$$\begin{aligned} &\dot{e}_1 = e_2 - 2l_1(l_{c3}m_3 + l_{c4}m_4)\delta(\dot{q}_1, q_2, e_5, e_7),\ \dot{e}_2 = e_3,\ \dot{e}_3 = e_4,\ \dot{e}_4 = w_2^{tr} - w_2^r, \\ &\dot{e}_5 = e_6,\ \dot{e}_6 = w_3^{tr},\quad \dot{e}_7 = e_8,\ \dot{e}_8 = w_4^{tr}. \end{aligned} \tag{53}$$

Recall, cf. *e.g.* [35], that the origin of the dynamical system (53) is globally finite-time stable, if it is Lyapunov stable and there exists positive-definite function of its state $T(e)$, called the settling-time function, such that any system trajectory $e(t)$ with the initial conditions $e(0) = e^0$ satisfies $e(t) = 0\ \forall t \geq T(e^0)$ and $e(t) \neq 0\ \forall t < T(e^0)$.

Proposition 15. *Consider (53) and define the following*

$$\begin{aligned} w_2^{tr} &= w_2^r + \textstyle\sum_{i=1}^4 K_i|e_i|^{\alpha_i}\mathrm{sign}(e_i), \qquad \alpha_1 = \tfrac{\alpha^2}{4-\alpha^2},\ \alpha_2 = \tfrac{\alpha^2}{3-\alpha^2},\ \alpha_3 = \tfrac{\alpha^2}{2-\alpha^2},\ \alpha_4 = \alpha^2, \\ w_3^{tr} &= K_5|e_5|^{\alpha_5}\mathrm{sign}(e_5) + K_6|e_6|^{\alpha_6}\mathrm{sign}(e_5), \qquad \alpha_5 = \tfrac{\alpha^3}{2-\alpha^3},\ \alpha_6 = \alpha^3, \\ w_4^{tr} &= K_7|e_7|^{\alpha_7}\mathrm{sign}(e_7) + K_8|e_8|^{\alpha_8}\mathrm{sign}(e_8), \qquad \alpha_7 = \tfrac{\alpha^3}{2-\alpha^3},\ \alpha_8 = \alpha^3. \end{aligned} \tag{54}$$

Let $K_1, \dots, K_8 \in \mathbb{R}$ are such that $s^4 + \sum_{i=1}^4 K_i s^{i-1}$, $s^2 + K_5 s + K_6$ and $s^2 + K_7 s + K_8$ are Hurwitz polynomials. Then there exists $\varepsilon \in (0,1)$ such that for every $\alpha^2, \alpha^3, \alpha^4 \in (1-\varepsilon, 1)$ the origin of the system (53) with $w_2^{tr}, w_3^{tr}, w_4^{tr}$ given by (54) is globally finite time stable.

Proof. By Proposition 8.1 of [35] there exists $\varepsilon_3, \varepsilon_4 \in (0,1)$ such that for every $\alpha^3 \in (1-\varepsilon_3, 1), \alpha^4 \in (1-\varepsilon_4, 1)$ the origin of the subsystem of (53) given its last four equations is globally finite-time stable. In such a way, considering arbitrary $e^0 \in \mathbb{R}^8$, there exists $T_{sub22}(e_5^0, \dots, e_8^0)$ such that the trajectory $e(t)$ of (53) with the initial conditions $e(0) = e^0$ satisfies $\forall t \geq T_{sub22}(e_5^0, \dots, e_8^0)$ that $e_5(t) = \dots = e_8(t) = 0$. Moreover, since the nonlinear term in the first equation of (53) is continuous, it is bounded on $[0, T_{sub22}(e_5^0, \dots, e_8^0)]$, and therefore $e_1(T_{sub22}(e_5^0, \dots, e_8^0)), \dots, e_4(T_{sub22}(e_5^0, \dots, e_8^0))$ are finite. Due to $\delta(\dot{q}_1, q_2, 0, 0) \equiv 0, \forall \dot{q}_1, q_2$, the subsystem of the first four equations of (53) becomes linear when $t \geq T_{sub22}$. By Proposition 8.1 of [35] then exists ε_2 such for $\alpha^2 \in (1-\varepsilon_2, 1)$ it is globally finite-time stable. As a consequence, there exists $T_{sub4}(e_1(T_{sub22}(e_5^0, \dots, e_8^0)), \dots, e_4(T_{sub22}(e_5^0, \dots, e_8^0)))$, such that $e_1(t) = \dots e_4(t) = 0$, $\forall t \geq T_{sub4}(e_1(T_{sub22}(e_5^0, \dots, e_8^0)), \dots, e_4(T_{sub22}(e_5^0, \dots, e_8^0)))$.

Choosing ε as the maximum of $\varepsilon_2, \varepsilon_3, \varepsilon_4 \in (0,1)$ completes the proof. □

The following theorem is stated for the non-switching torsos, the switching torsos case is analogous, with straightforward minor adaptations, cf. Theorems 3 and 7.

Theorem 16. *Consider DTB (6)–(8), its double support configurations $q^+ = [q_1^+, \dots, q_4^+]^\top \in \mathbb{R}^4$, $q^- = [q_1^-, \dots, q_4^-]^\top \in \mathbb{R}^4$ and $T > 0$. Denote by $\xi^+ = [\xi_1^+, \xi_3^+, \xi_5^+, \xi_7^+]^\top$, $\xi^- = [\xi_1^-, \xi_3^-, \xi_5^-, \xi_8^-]^\top$ the images of $q^+ \in \mathbb{R}^4$, $q^- \in \mathbb{R}$, respectively, by the mapping (15). Further, let the above configurations $q^+ \in \mathbb{R}^4$, $q^- \in \mathbb{R}^4$ are such that $\xi_5^+ = \dots = \xi_8^+ = 0$, $\xi_5^- = \dots = \xi_8^- = 0$ and $\xi_2^+, \xi_4^+ \xi_2^-, \xi_4^-$ satisfy (49) for some real a, b. Denote by $\xi^r(t)$ the solution of (19) given by (51) (existing due to Lemma 13) and assume that the image of $\xi^r(t)$ by the inverse of (15) belongs $\forall t \in [0,T]$ to $Q \times \mathbb{R}^7$, Q is given by (37). Define*

$$\begin{bmatrix} u_2^{tr} \\ u_3^{tr} \\ u_4^{tr} \end{bmatrix} = \mathscr{S}\mathscr{D}_{q^0}^{-1}\left[\begin{bmatrix} w_2^{tr} + \dot{q}^\top \nabla^\top \nabla G_1(q)\dot{q} \\ w_3^{tr} - \theta(q_2, \dot{q}_2) \\ w_4^{tr} \end{bmatrix} - \Theta(q, \dot{q})\right] + \begin{bmatrix} C_2(q,\dot{q}) + G_2(q) \\ C_3(q,\dot{q}) + G_3(q) \\ C_4(q,\dot{q}) + G_4(q) \end{bmatrix}, \tag{55}$$

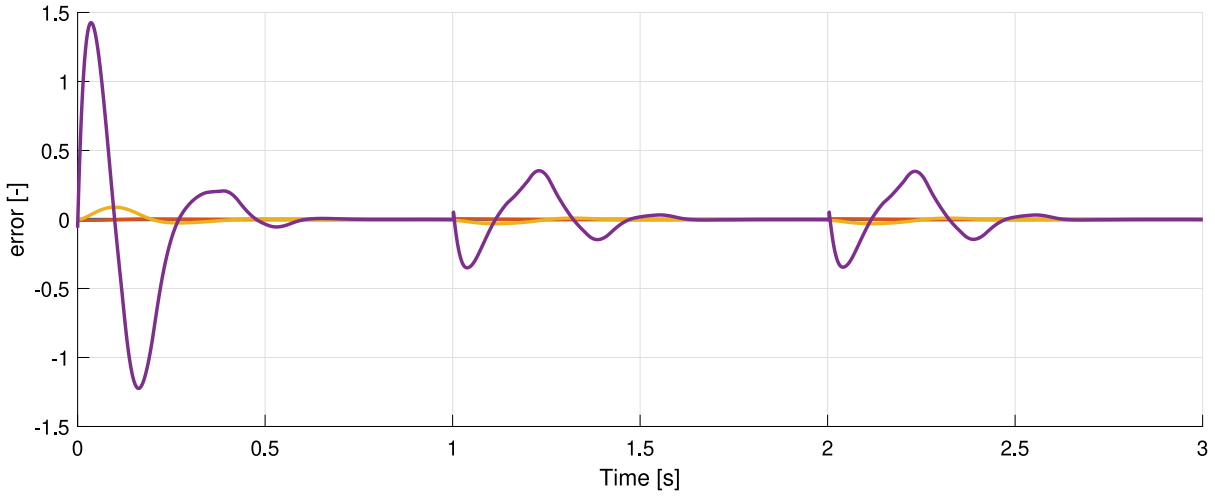

Fig. 5. The tracking errors e_1, e_2, e_3 and e_4 - the blue, red, yellow and violet lines, respectively.

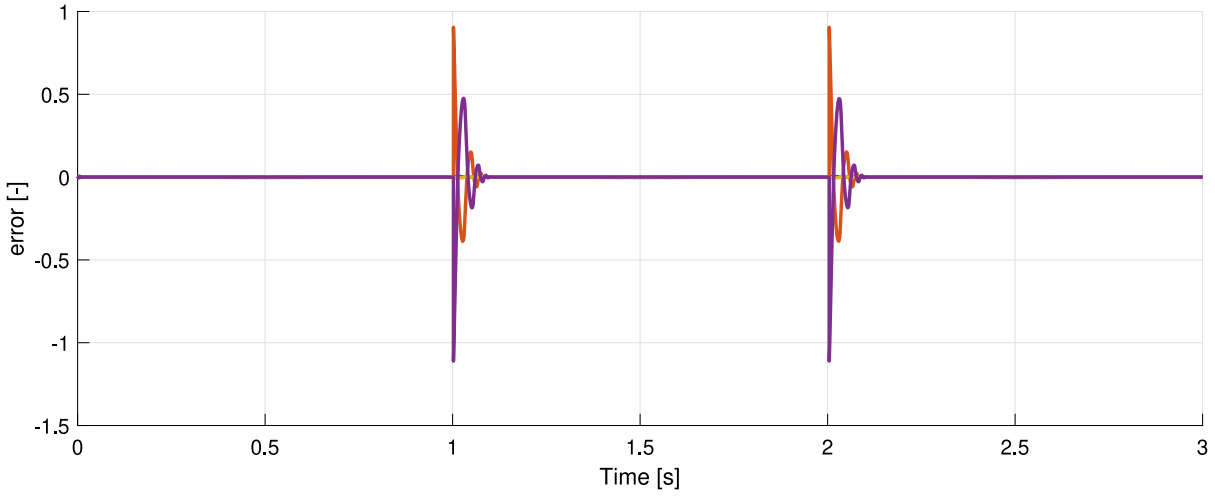

Fig. 6. The tracking errors e_5, e_6, e_7 and e_8 - the blue, red, yellow and violet lines, respectively.

where $\mathscr{S}$ is given by (29), $\mathscr{D}_{q^0}$ by (12), $w_2^{tr}, w_3^{tr}, w_4^{tr}$ are given by (54) with $\xi(t)$ substituted from (15), $\theta(q,\dot{q})$ by (15), $\Theta(q,\dot{q})$ by (22) and $w_2^r = a + bt$. Then the following holds.

1. *Trajectory $q^r(t)$ of (6)–(8) with the input (55) and the initial condition $q^r(0) = q^+$ is unique, exists $\forall t \in [0,T]$ and satisfies $q^r(T) = q^-$. Moreover, its image $\xi^r(t)$ by the mapping (15) modified by (34) $\forall t \in [0,T]$ satisfies $\xi_5^r(t) = \cdots = \xi_8^r(t) = 0$.*

2. *There exists a neighborhood $\mathscr{N}_{q^+}$ of $q^+ \in \mathbb{R}^4$ and a settling-time function $\widehat{T} : \mathscr{N}_{q^+} \mapsto [0,T)$ such that any trajectory $q(t)$ of (6)–(8) with the input (55) and the initial condition $q(0) = q^0 \in \mathscr{N}_{q^+}$ satisfies $q(t) = q^r(t),\ \forall t \geq \widehat{T}(q^0)$.*

Proof. Straightforward using (21), (32), Theorem 3, Lemma 13 and Proposition 15. □

Remark 17. Based on Theorem 16 the DTB multi-step walking can be designed as follows:

1. Find a smooth connected curve in $\mathbb{R}^3$ connecting $[q_2^+, q_3^+, q_4^+]^\top$ and $[q_2^-, q_3^-, q_4^-]^\top$ such that along that curve for $\xi_5(t), \xi_7(t)$ given by (15)–(34) it holds $\xi_5(t) \equiv \xi_7(t) \equiv 0$. This task is **a very basic necessary applicability condition**, indeed, it means that there exists a connected component of the pre-image of the set where the almost linear form (19) becomes linear and containing both q^+ and q^-. By Theorem 3 this task is explicitly solvable for the switching torsos case if (16) holds. Obviously, (16) still gives a lot of variety for a sensible swing phase design. Indeed, adapting torsos spreading to legs spreading (dependently on the balancing factor $\beta := l_{c2} m_2 l_{c3}^{-1} m_3^{-1} = l_{c1} m_1 l_{c4}^{-1} m_4^{-1}$ between torsos and legs) seems to be quite natural.

2. Having curve found above, its lift to $\mathbb{R}^4$ by Cartesian product with q_1-component should contain nonempty set where $\det \mathscr{D}_{sw}(q_1, q_2, q_3, q_4) \neq 0$, this is still another **necessary applicability condition**, without it, what follows would be obviously useless.

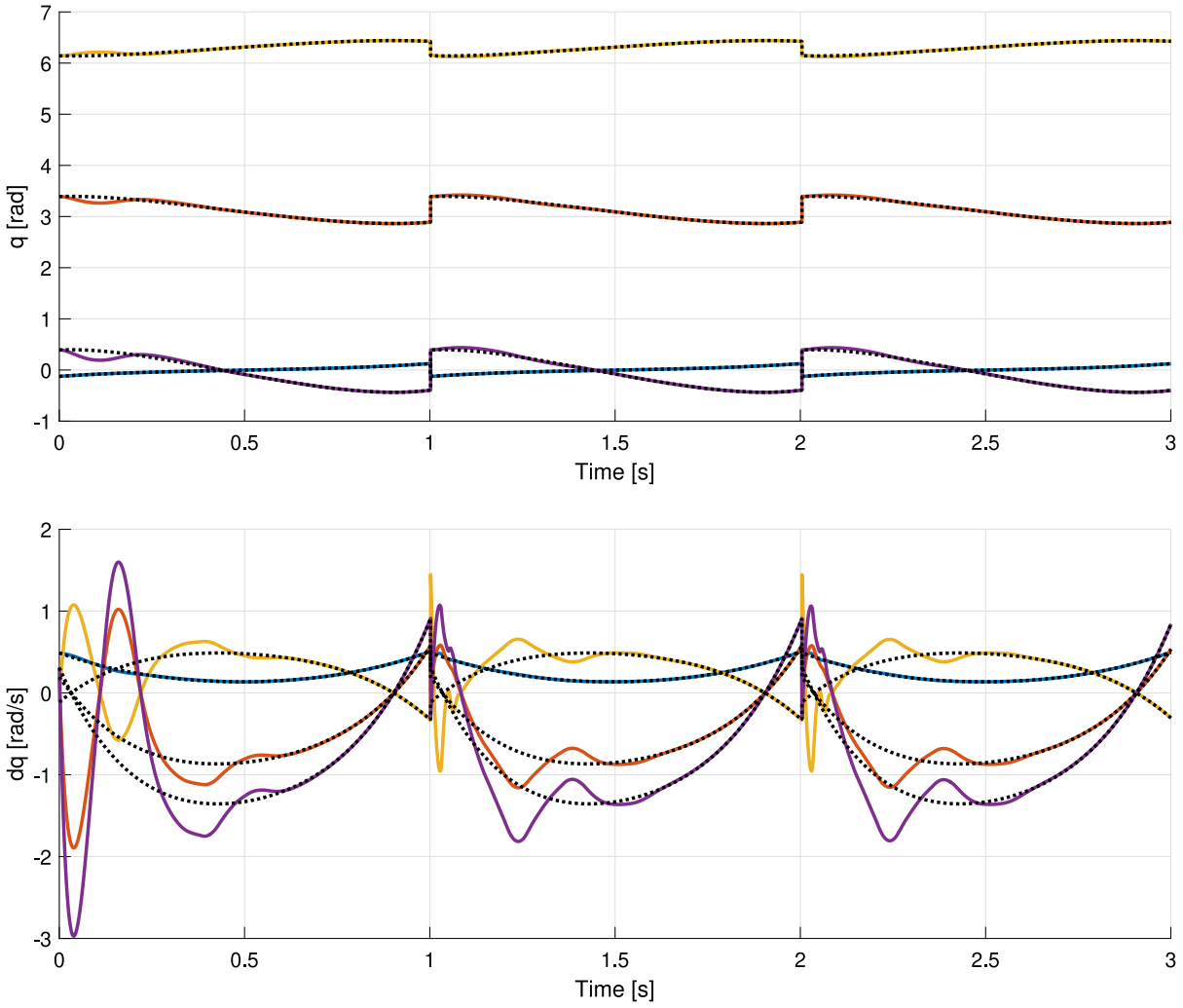

Fig. 7. The switching torsos case. Up: the angles, down the angular velocities. The references are dotted, the trajectories tracking them are full lines. The blue, red, yellow and violet lines represent q_1, q_2, q_3, q_4, respectively. Three steps, each of them taking 1s, are shown. Further steps are identical with the third one and are not shown.

If this necessary condition holds, one can try to compute trajectory of (6)–(8) starting at q^+ with the input given by (55) and check $\det \mathscr{D}_{sw}(q_1, q_2, q_3, q_4) \neq 0$ along it. If true, the image of $\xi^r(t)$ by the inverse of (15) belongs $\forall t \in [0, T]$ to $Q \times \mathbb{R}^7$, Q given by (37), and Theorem 16 is applicable. Note, that in practical computations the violation of $\det \mathscr{D}_{sw}(q_1, q_2, q_3, q_4) \neq 0$ results in collapse of that computations since (55) contains the inverse of $\mathscr{D}_{sw}$. In case of collapse, one can vary β and q_2^+, q_3^+, q_4^+ subject to constraint (36) and repeat the above. Such an approach is quite feasible as demonstrated by numerical simulations later on.

3. If previous two steps are successful, as already noted, Theorem 16 is applicable, yet its claim **2.** is only local and to guarantee finite settling time less than T (the time duration of the step), the initial tracking errors might be required to be rather small. This aspect is further complicated by the fact that there is no hybrid invariance of relation $\xi_5 = \xi_7 = 0$, *i.e.* the impact impulsively creates some *ad hoc* tracking errors in e_5, e_7 at the beginning of the next step. Settling time can be adjusted by enhancing design parameters $K_1, \ldots, K_8$, $\alpha_1, \ldots, \alpha_4$, yet, it is well known that this leads to larger initial error peak, which could take trajectory $\xi^{tr}(t)$ outside the image of $Q \times \mathbb{R}^7$, where transformations (15) are defined.

4. Fortunately, there are some aspects enabling to handle those ad hoc tracking errors in e_5, e_7 at the beginning of the next step. First, dynamics of $e_5, \ldots, e_8$ is fully linear, independent from $e_1, \ldots, e_4$, and the respective transformation components are valid in a wide range. As a consequence, peaking phenomenon in $e_5, \ldots, e_8$ is not an issue and their ad hoc errors can be quickly put to zero. Further, the initial conditions of $e_1, \ldots, e_4$ at the beginning of the next step are zero, since the reference $\xi^r(t)$ solves Problem 11, and the only nonlinearity $\delta(\dot{q}_1, q_2, e_5, e_7)$ at the first equation is globally Lipschitz with $\delta(\dot{q}_1, q_2, 0, 0) \equiv 0$. It affects $\dot{e}_1$ only when e_5, e_7 are nonzero, the latter are put to zero in arbitrary small time for price of higher peaking, yet, it is known that integral of errors are not growing (peak is higher, but narrower), this stems from the essence on the finite-time stabilization technique in [35] shaping the

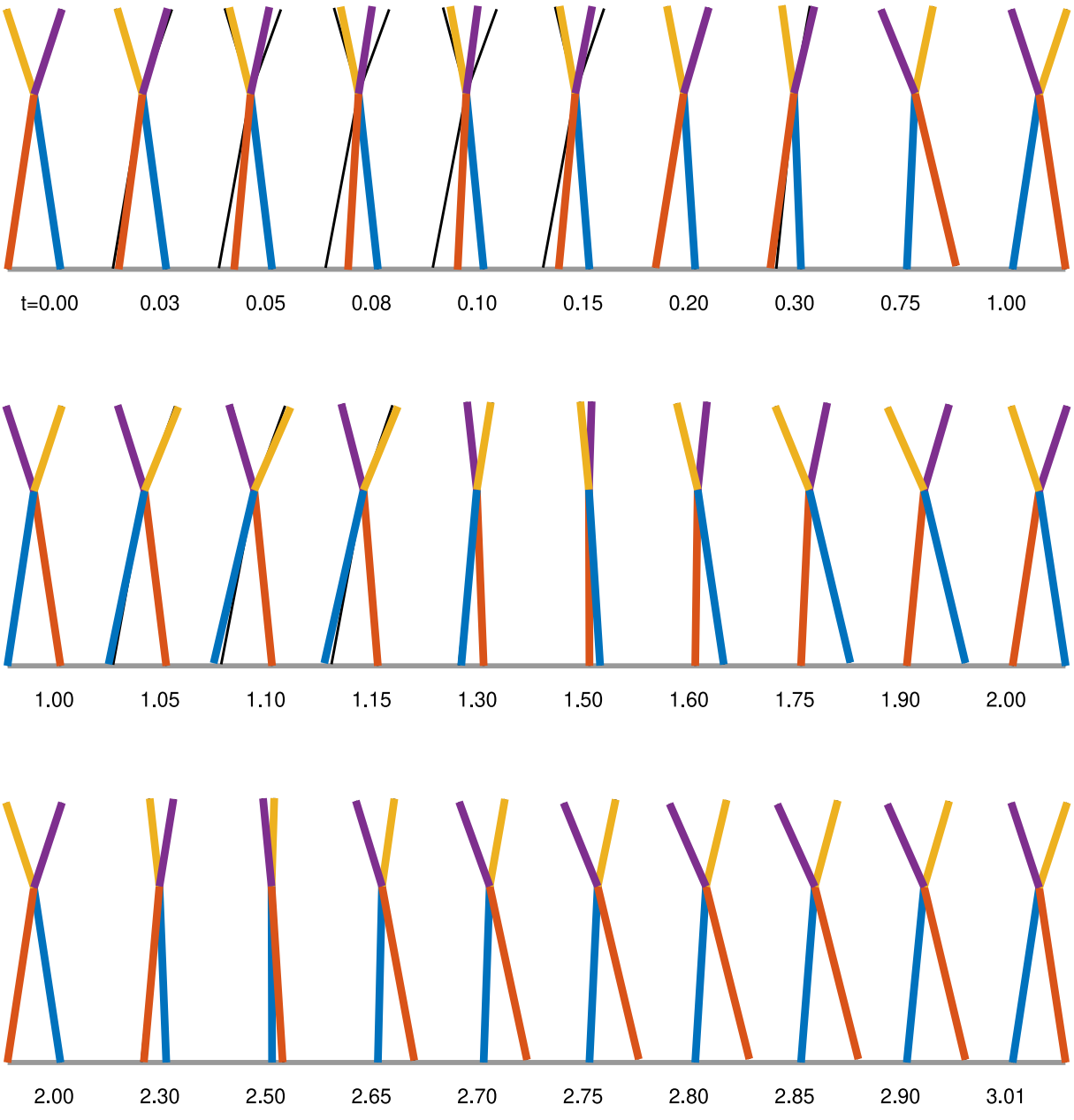

Fig. 8. The snaps of the animation of the DTB hybrid sustainable walking — the switching torsos case. The time moments of the snaps are shown below the horizontal walking surface. The black thin full line DTB represents the reference to be tracked. The colored torso represents the controlled DTB. Legs are red and blue, while torsos yellow and violet to facilitate the switching of torsos and legs demonstration. The switching of the torsos is visible approximately at time moments $t = 0.5, 1.5, 2.5$ coinciding as expected theoretically with the legs switching. Three steps only are shown, while the first and the second steps demonstrate the decreasing tracking errors, during the third step reference already coincides with the controlled DTB. The subsequent steps repeat exactly the third one and therefore are not shown for the space reasons.

response by the appropriate dilation. This indicates possible ways for precise theoretical proof, which is outside the scope and the length of the current paper.

5. The previous theoretical sketch is nicely illustrated by simulations in Figs. 5, 6 showing tracking errors in linearized coordinates. The time duration of steps $T = 1$ and three steps are shown. Both Figs. 5 and 6 have the same dimensions, so time courses can be easily compared. At the beginning of the first step there is some added random tracking error. Clearly, by the end of each step tracking error is zero, after impact first four components, cf. Fig. 5 stay zero, while the last four, cf. 6 become impulsively nonzero. Yet, they are quickly pushed to zero, meanwhile they generate some error in first four equations thanks to $\delta(\dot{q}_1, q_2, e_5, e_7)$. Since meanwhile $\delta(\dot{q}_1, q_2, e_5, e_7) = 0$, the finite time linear controller for the first four integrators starts to work and push $e_1, \ldots, e_4$

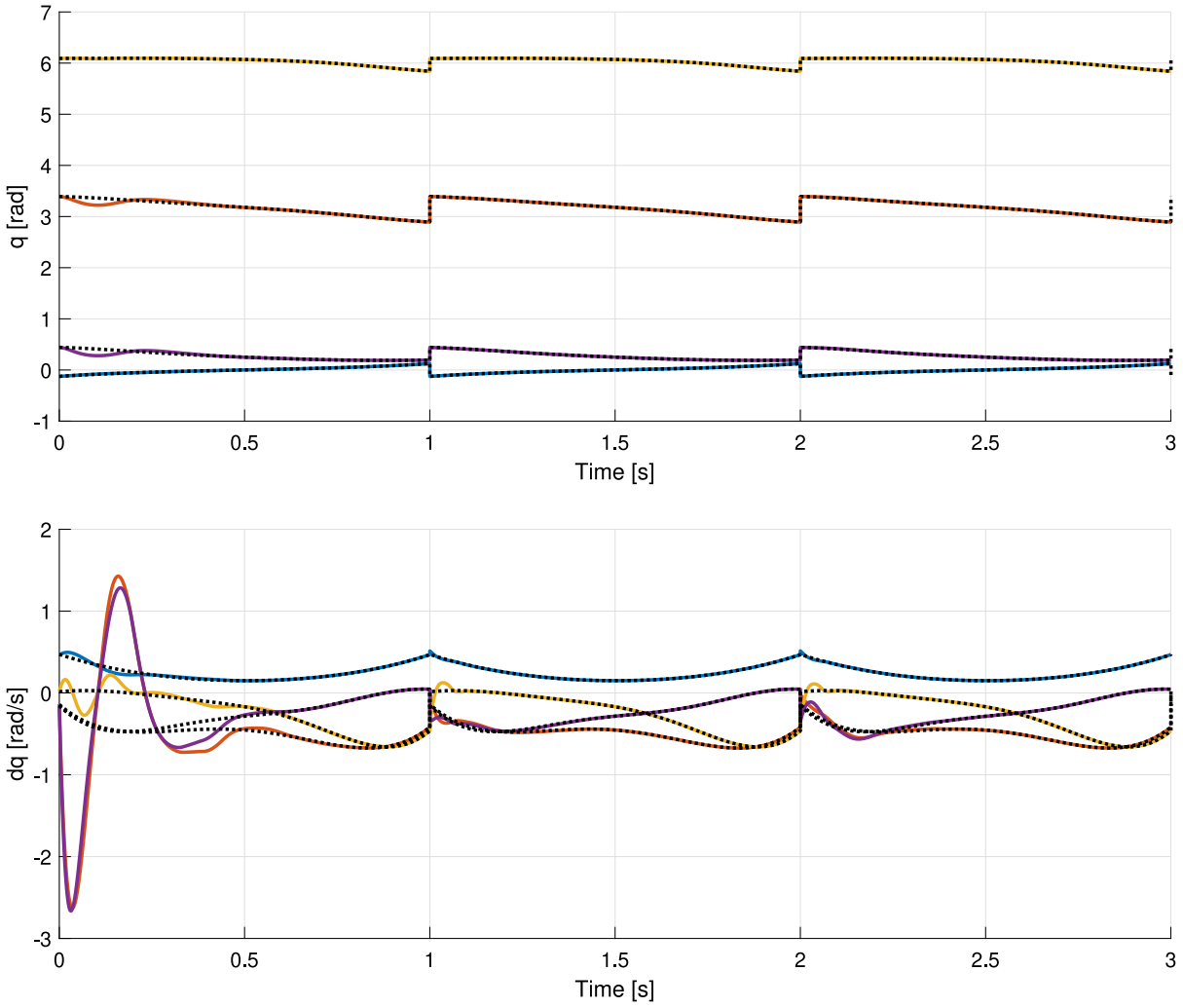

Fig. 9. The non-switching upward torsos case. Up: the angles, down the angular velocities. The references are dotted, the trajectories tracking them are full lines. The blue, red, yellow and violet lines represent q_1, q_2, q_3, q_4, respectively. Three steps, each of them taking 1s, are shown. Further steps are identical with the third one and are not shown.

to zero as well. Note interesting fact that starting the second step trajectory is, indeed, the cyclic one, though it is not the hybrid invariant one.

4.4. Simulations

First, note that the matrix $\mathscr{C}$, given by (48) and needed for the controller (55) design, is generically nonsingular with respect to the choice of mechanical parameters, initial and final spreading of legs and torsos at double support stance configurations, *etc.* As a consequence, in practical simulations it never happened to be singular, thereby facilitating selection of these parameters motivated by other purposes. Further, as noted when commenting Fig. 1, the mechanical parameters in theoretical models (6)–(8) with massless links and lumped masses at their CM's are virtual re-computations of the real laboratory model with distributed masses: homogeneous links of nonzero masses, added masses at some places at the links *etc.* As for the design actually only the balancing factor $\beta := l_{c2}m_2l_{c3}^{-1}m_3^{-1} = l_{c1}m_1l_{c4}^{-1}m_4^{-1}$ between torsos and legs matters, we skip those particular values in the sequel.

Three types of walking-like movement of the DTB were extensively simulated and tested namely, switching torsos case, non-switching upward torsos case and non-switching downward torsos case.

1. Switching torsos case. It is demonstrated here by Fig. 7 where trajectories are shown and by the animation in Fig. 8. One can clearly see the torsos switching due to their coloring. As expected theoretically, the torsos switching occurs at the same time moment as the legs switching. In this case, $\beta = 2.75$ and the equality (36) holds at the beginning of the step ensuring the switching.

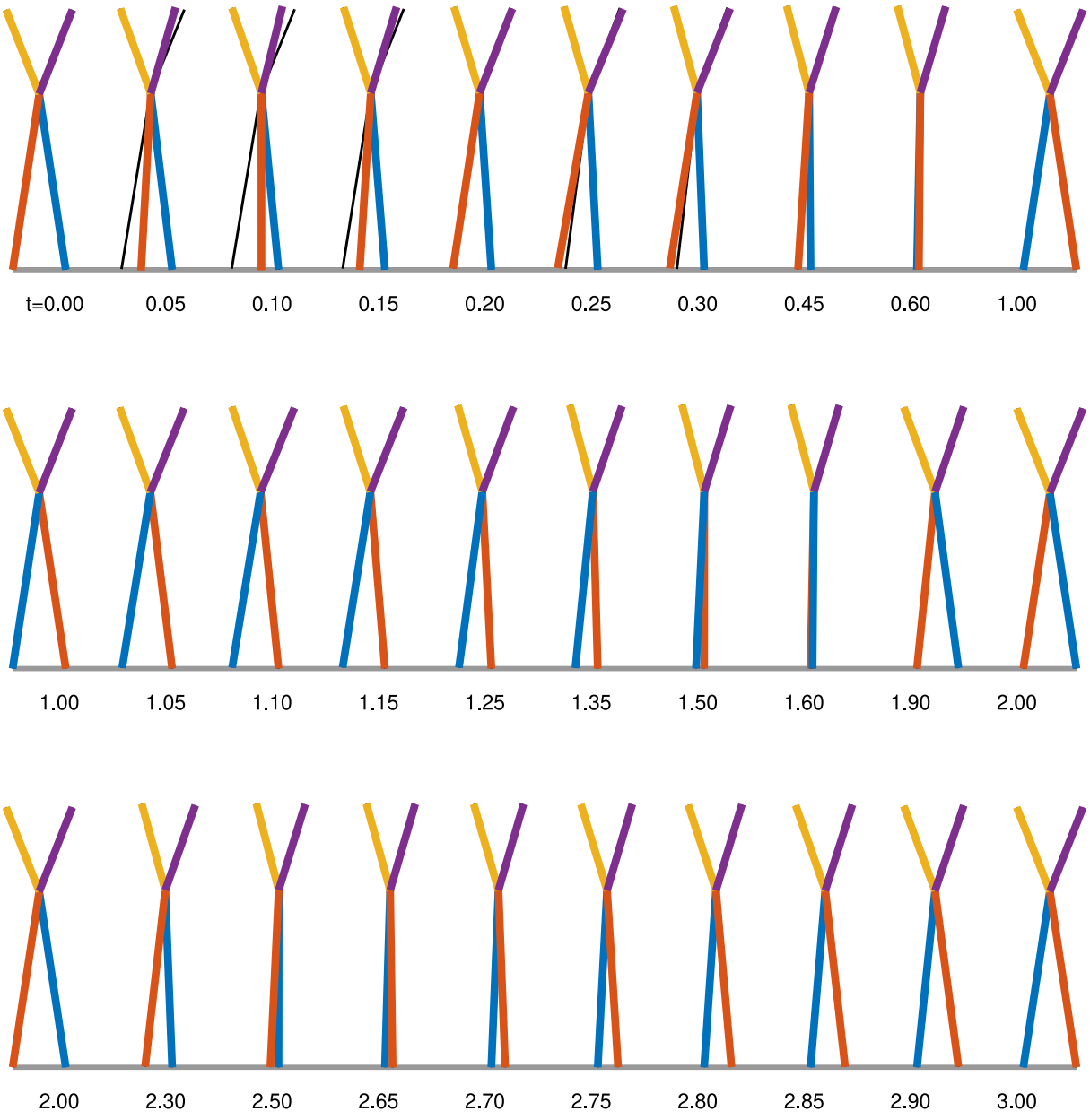

Fig. 10. The snaps of the animation of the DTB hybrid sustainable walking — the non-switching upward torsos case. The time moments of the snaps are shown below the horizontal walking surface. The black thin full line DTB represents the reference to be tracked. The colored torso represents the controlled DTB. Legs are red and blue, while torsos yellow and violet to facilitate the observation that torsos do not switch while legs are mutually switching. When legs are switching, the relative torsos angle is the smallest one. Three steps only are shown, while the first and the second steps demonstrate the decreasing tracking errors, during the third step reference already coincides with the controlled DTB. The subsequent steps repeat exactly the third one and therefore are not shown for the space reasons.

It is nicely seen in Fig. 7 that impact violates visibly the reference tracking for velocities, but error for angles grows almost invisibly and is quickly suppressed.

2. Non-switching upward torsos case. It is demonstrated here by Fig. 9 where tracking trajectories are shown in detail and the animation in Fig. 10. In this case, $\beta = 2$ and only the **inclusion** (16) is required (unlike the switching torsos case where the **equality** (36) is required) for the configuration angles at the beginning of the step. Non-switching upward torsos case controller applied to an initial configuration satisfying (36) (being kind of boundary case of (16), but violating it) would result in torsos coinciding, but then their receding back, requiring unrealistic infinite control action. Indeed, the torsos would coincide each with other having nonzero velocity, so receding would require jump in velocities. On the contrary, if (16) holds, there is always nonzero angle between torsos,

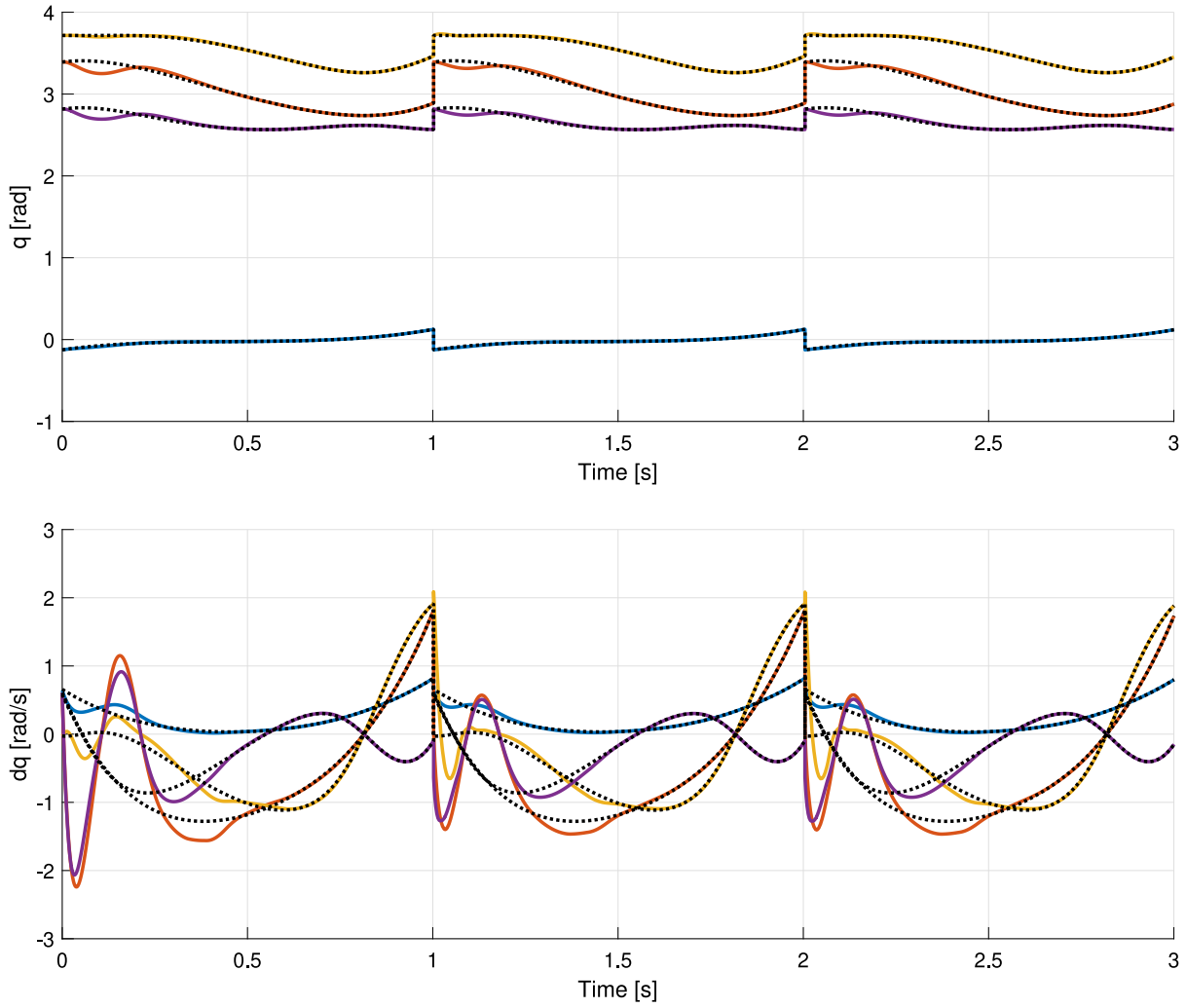

Fig. 11. The non-switching downward torsos case. Up: the angles, down the angular velocities. The references are dotted, the trajectories tracking them are full lines. The blue, red, yellow and violet lines represent q_1, q_2, q_3, q_4, respectively. Three steps, each of them taking 1s, are shown. Further steps are identical with the third one and are not shown.

when they start to recede, and at that respective moment their velocities are zero and go smoothly back. Notably, jump in tracking errors at the impacts is in Fig. 9 much smaller than in Fig. 7.

3. Non-switching downward torsos case. It is demonstrated here by Fig. 11, where tracking trajectories are shown in detail and the animation in Fig. 12. In this case, $\beta = 1.4571$ and only the inclusion (16) is required at the beginning of the step, the only difference with respect the non-switching upward case is just that downward case is "deeply inside" the inclusion (16), so that the torsos start to recede being far away from possible coinciding and even staying downward all the time. Animation of the downward torsos resemble hands, nevertheless, a possible idea of the torsos going more down and switch each other at the downward position contradicts to the idea of constant value of $d_{11}(q)$. Indeed, realize that d_{11} represents (up to multiplication by some physical constants) the moment of inertia of the overall DTB configuration with respect to the pivot point. Moreover, for the torsos coinciding downward there is always a singularity of the transformation (15).

As a matter of fact, all animations nicely show the fundamental mechanical idea about the almost linear form (19). This form becomes exactly linear along target trajectory constructed inside the invariant constrained dynamics where $\xi_5 = 0$ and $\xi_7 = 0$. The condition $\xi_5 = 0$ is equivalent to $d_{11}(q)$ being constant. Mechanically that simply means that the moment of inertia with respect to the pivot point is constant along overall target trajectory. Such a feature can be noticed in all animations — torsos spreading actually compensate the change of that moment of inertia caused by legs mutual closing, and vice-versa. In particular, the balancing parameter β (10) influences the measure of torsos spreading, smaller β require smaller torsos spreading and vice-versa. Indeed, recall that β express ratio between inertia of legs and torsos.

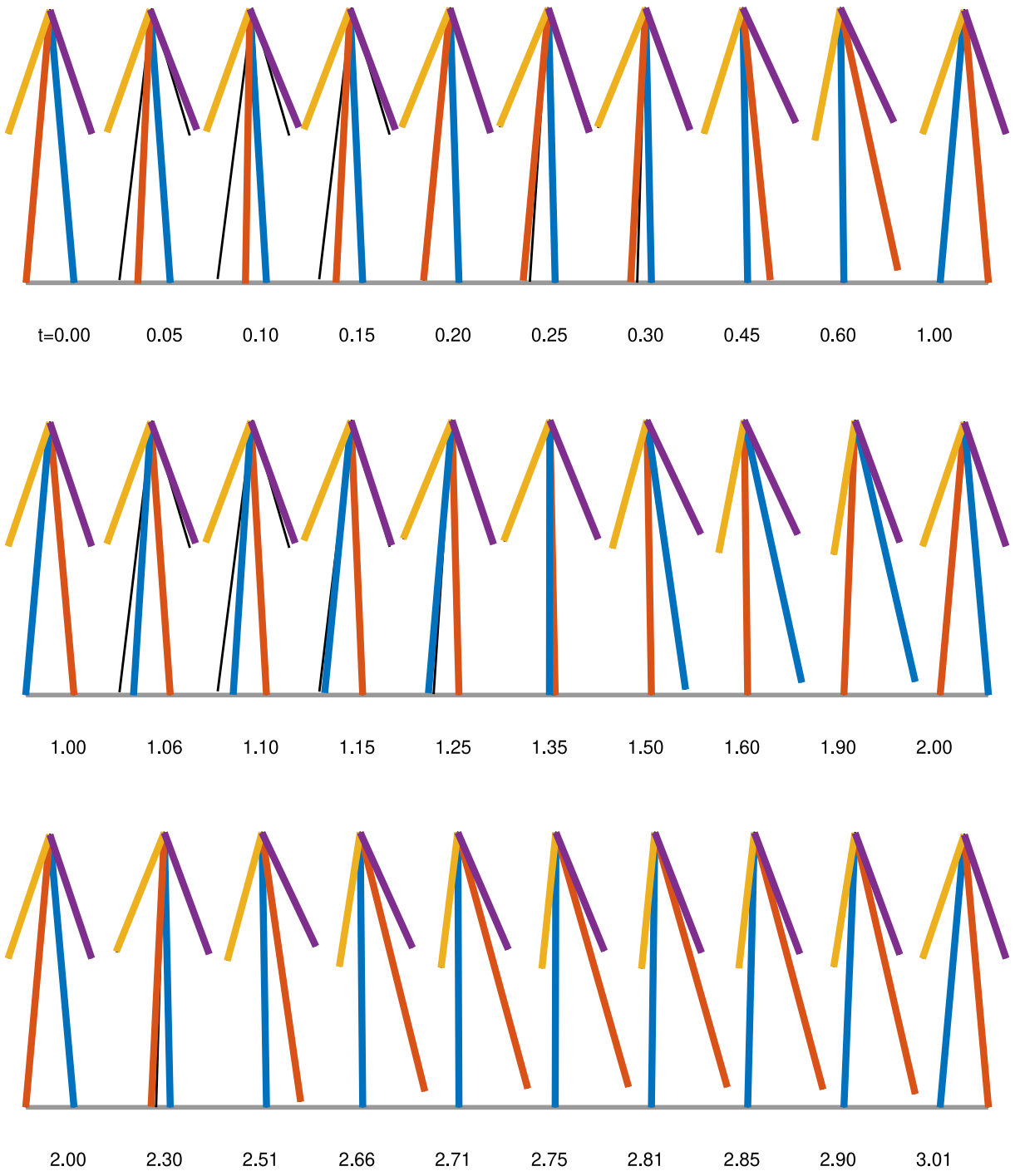

Fig. 12. The snaps of the animation of the DTB hybrid sustainable walking — non-switching downward torsos case. The time moments of the snaps are shown below the horizontal walking surface. The black thin full line torso represents the reference to be tracked. The colored torso represents the controlled DTB. Legs are red and blue, while torsos yellow and violet to demonstrate that torsos do not switch while legs do switch. The relative torsos angle is the biggest at the time moment of legs switching. Three steps only are shown, while the first and the second steps demonstrate the decreasing tracking errors, during the third step reference already coincides with the controlled DTB. The subsequent steps repeat exactly the third one and therefore are not shown for the space reasons.

5. Conclusions

This paper shows that the Lagrangian model of the double torso biped is smoothly state and feedback equivalent to the 8-dimensional almost linear form with 3 virtual controlled inputs. Moreover, the only nonlinearity vanishes on a rich collection of trajectories belonging to its four dimensional linear subspace being forward invariant when 2 of those virtual inputs are set to be identically zero. The multi-step walking design using the favorable properties of the resulting linear systems was presented and successfully tested in simulations. The mentioned four dimensional linear subsystem corresponds in reality to a certain synchronization between legs and torsos keeping the moment of inertia of the double torso biped with respect to pivot point constant during the target swing phase step. As torsos imitate in a certain simplified way the role of the hands during the walking, the above ideas suggest interesting and natural interpretation of the balancing role of the hands during the walking.

Future research will be devoted to the generalization of the paper results to the walking-like system having legs with knees and single torso with two hands.

CRediT authorship contribution statement

Sergej Čelikovský: Formal analysis, Funding acquisition, Investigation, Project administration, Writing – original draft. **Milan Anderle:** Investigation, Software, Validation, Visualization, Writing – review & editing.

Declaration of competing interest

The authors declare that they have no known competing financial interests or personal relationships that could have appeared to influence the work reported in this paper.

Acknowledgment

Supported by the Czech Science Foundation grant No. 21-03689S.

References

[1] I. Fantoni, R. Lozano, Non-linear Control of Underactuated Mechanical Systems, Springer Verlag, Heidelberg, 2002, p. 295.
[2] T. Horibe, N. Sakamoto, Nonlinear optimal control for swing up and stabilization of the acrobot via stable manifold approach: Theory and experiment, IEEE Trans. Control Syst. Technol. 27 (6) (2019) 2374–2387.
[3] Q. Luo, C. Chevallereau, Y. Aoustin, Walking stability of a variable length inverted pendulum controlled with virtual constraints, Int. J. Hum. Robot. 16 (6) (2019) 1950040–1–1950040–24.
[4] B. Beigzadeh, S.A. Razavi, Dynamic walking analysis of an underactuated biped robot with asymmetric structure, Int. J. Hum. Robot. 18 (04) (2021) 2150014.
[5] J. Tian, C. Wei, Y. Zhao, Singular configurations and underactuated balance control for biped robot with point contact, Int. J. Hum. Robot. 17 (06) (2020) 2050022.
[6] X. Luo, D. Xia, C. Zhu, Impact dynamics-based torso control for dynamic walking biped robots, Int. J. Hum. Robot. 15 (03) (2018) 1850004.
[7] E. Selim, M. Alci, Walking speed control of planar bipedal robot with phase control, Int. J. Hum. Robot. 19 (06) (2022) 2250023.
[8] E. Westervelt, J. Grizzle, C. Chevallereau, J. Choi, B. Morris, Feedback Control of Dynamic Bipedal Robot Locomotion, CRC Press, 2007.
[9] C. Chevallereau, G. Bessonnet, G. Abba, Y. Aoustin, Bipedal Robots: Modeling, Design and Walking Synthesis, Wiley-ISTE, 2009.
[10] G. Song, M. Zefran, Stabilization of hybrid periodic orbits with application to bipedal walking, in: Proc. of the 2006 American Control Conference, Minneapolis, Minnesota, 2006, pp. 2504–2509.
[11] G. Song, M. Zefran, Underactuated dynamic three-dimensional bipedal walking, in: Proc. of the 2006 IEEE Int. Conf. on Robotics and Automation, ICRA, Orlando, Florida, 2006, pp. 854–859.
[12] A. Majumdar, A. Ahmadi, R. Tedrake, Control design along trajectories with sums of squares programming, in: Proceedings of the 2013 IEEE International Conference on Robotics and Automation, ICRA, Karlsruhe, Germany, 2013, pp. 4054–4061.
[13] J. Grizzle, C. Chevalereau, R. Sinnet, A. Ames, Models, feedback control and open problems of 3D bipedal robotic walking, Automatica 50 (8) (2014) 1955–1988.
[14] P. La Herra, A. Shiriaev, L. Freidovich, U. Mettin, S. Gusev, Stable walking gaits for a three-link planar biped robot with one actuator, IEEE Trans. Robot. 29 (3) (2013) 589–601.
[15] V.V. Kozlov, The dynamics of systems with servoconstraints. I, Regul. Chaotic Dyn. 20 (3) (2015) 205–224.
[16] S. Čelikovský, M. Anderle, Collocated virtual holonomic constraints in Lagrangian systems and their application, in: American Control Conference 2016, Boston, MA, USA, 2016, pp. 6030–6035.
[17] M. Maggiori, L. Consolini, Virtual holonomic constraints for Euler–Lagrange systems, IEEE Trans. Automat. Control 58 (4) (2013) 181–185.
[18] A. Mohammadi, M. Maggiore, L. Consolini, When is a Lagrangian system with virtual holonomic constraints Lagrangian, in: Proc. of the 9th IFAC NOLCOS, Toulouse, France, 2013, pp. 512–517.
[19] S. Čelikovský, Flatness and realization of virtual holonomic constraints, in: Proc. of the 5th IFAC Workshop on Lagrangian and Hamiltonian Methods for Non Linear Control, Lyon, France, 2015, pp. 25–30.
[20] S. Čelikovský, M. Anderle, Hybrid invariance of the collocated virtual holonomic constraints and its application in underactuated walking, in: IFAC-PapersOnLine, IFAC NOLCOS 2016, Vol. 49–18, Monterey, CA, USA, 2016, pp. 802–807.
[21] L. Cambrini, C. Chevallereau, C. Moog, R. Stojic, Stable trajectory tracking for biped robots, in: Proceedings of the 39th IEEE Conference on Decision and Control, Sydney, NSW, Australia, 2000, pp. 4815–4820.
[22] M. Anderle, S. Čelikovský, D. Henrion, J. Zikmund, Advanced LMI based analysis and design for Acrobot walking, Internat. J. Control 83 (8) (2010) 1641–1652.
[23] S. Čelikovský, M. Anderle, C. Moog, Embedding the Acrobot into a general underactuated n-link with application to novel walking design, in: Proceedings of the Europen Control Conference, ECC 2013, Zurich, Switzerland, 2013, pp. 682–689.

[24] S. Čelikovský, M. Anderle, Collocated virtual holonomic constraints in Hamiltonian formalism and their application in the underactuated walking, in: Proceedings of the 11th Asian Control Conference, (ASCC) 2017, Gold Coast, Australia, 2017, pp. 192–197.
[25] S. Čelikovský, M. Anderle, On the Hamiltonian approach to the collocated virtual holonomic constraints in the underactuated mechanical systems, in: Proceedings of the 4th International Conference on Advanced Engineering Theory and Applications, AETA, Ho Chi Min City, Vietnam, 2017.
[26] R. Olfati-Saber, Normal forms for underactuated mechanical systems with symmetry, IEEE Trans. Autom. Control 47 (2) (2002) 305–308.
[27] J. Grizzle, C. Moog, C. Chevallereau, Nonlinear control of mechanical systems with an unactuated cyclic variable, IEEE Trans. Autom. Control 50 (5) (2005) 559–576.
[28] S. Čelikovský, M. Anderle, Exact feedback linearization of the collocated constrained dynamics of the three-link with adjustable torso and its application in the underactuated planar walking, in: 2019 IEEE 15th Int. Conf. on Control and Automation, ICCA, Edinburg, Scotland, 2019, pp. 1289–1295.
[29] S. Čelikovský, M. Anderle, Chain of four integrators as a possible essence of the under-actuated planar walking, IFAC-PapersOnLine 54 (14) (2021) 60–65.
[30] J. Grizzle, G. Abba, F. Plestan, Asymptotically stable walking for biped robots: Analysis via systems with impulse effects, IEEE Trans. Autom. Control 46 (1) (2001) 51–64.
[31] M. Wisse, A. Schwab, F. van der Helm, Passive dynamic walking model with upper body, Robotica 22 (6) (2004) 681–688.
[32] S. Čelikovský, M. Anderle, On the equivalence of the three-link to the almost linear form, in: 2022 IEEE Workshop on Complexity in Engineering, COMPENG, Florence, Italy, 2022, pp. 1–5.
[33] R. Ortega, A. Loria, P. Nicklasson, H. Sira-Ramírez, Passivity-based Control of Euler–Lagrange Systems, Springer Verlag, Heidelberg, 1998, p. 543.
[34] I. Sandberg, Global inverse function theorems, IEEE Trans. Circuits Syst. CAS-27 (1980) 998–1004.
[35] S. Bhat, D.S. Bernstein, Geometric homogeneity with applications to finite-time stability, Math. Control Signals Systems 17 (2005) 101–127.